

## Characterization of VU0468554, a new selective inhibitor of cardiac GIRK channels

Allison Anderson<sup>1</sup>, Baovi N. Vo<sup>1</sup>, Ezequiel Marron Fernandez de Velasco<sup>2</sup>, Corey R. Hopkins<sup>3</sup>,  
C. David Weaver<sup>4,5</sup>, Kevin Wickman<sup>2\*</sup>

<sup>1</sup> Graduate Program in Pharmacology, University of Minnesota, Minneapolis, MN

<sup>2</sup> Department of Pharmacology, University of Minnesota, Minneapolis, MN

<sup>3</sup> Department of Pharmaceutical Sciences, College of Pharmacy, University of Nebraska  
Medical Center, Omaha, NE

<sup>4</sup> Departments of Pharmacology and Chemistry, Vanderbilt University, Nashville, TN

<sup>5</sup> Institute of Chemical Biology, Vanderbilt University, Nashville, TN

## Running title

### *A new inhibitor of cardiac GIRK channels*

#### \* **Corresponding author**

Kevin Wickman, PhD  
University of Minnesota  
Department of Pharmacology  
6-120 Jackson Hall  
321 Church Street SE  
Minneapolis, MN 55455  
Tel: (612) 624-5966  
email: wickm002@umn.edu

<b>Text Pages</b>	29
<b>Tables</b>	0
<b>Figures</b>	4
<b>References</b>	52
<b>Words</b>	
Abstract	174
Introduction	681
Discussion	1179

#### **Non-standard abbreviations**

A <sub>1</sub> R	adenosine 1 receptor
AF	atrial fibrillation
APD	action potential duration
AV	atrioventricular
CCh	carbachol
ERP	effective refractory period
GIRK	G protein-gated inwardly rectifying K <sup>+</sup>
HR	heart rate
HRV	heart rate variability
RGS6	Regulator of G protein Signaling 6
SAN	sinoatrial node
VU554	VU0468554

## ABSTRACT

**G protein-gated inwardly rectifying K<sup>+</sup> (GIRK/Kir3) channels are critical mediators of excitability in the heart and brain. Enhanced GIRK channel activity has been implicated in the pathogenesis of supraventricular arrhythmias, including atrial fibrillation. The lack of selective pharmacological tools has impeded efforts to investigate the therapeutic potential of cardiac GIRK channel interventions in arrhythmias. Here, we characterize a recently identified GIRK channel inhibitor, VU0468554. Using whole-cell electrophysiological approaches and primary cultures of sinoatrial nodal cells and hippocampal neurons, we show that VU0468554 more effectively inhibits the cardiac GIRK channel than the neuronal GIRK channel. Concentration-response experiments suggest that VU0468554 inhibits G $\beta\gamma$ -activated GIRK channels in non-competitive, and potentially uncompetitive, fashion. In contrast, VU0468554 competitively inhibits GIRK channel activation by ML297, a GIRK channel activator containing the same chemical scaffold as VU0468554. In the isolated heart model, VU0468554 partially reversed carbachol-induced bradycardia in hearts from wild-type mice, but not *Girk4*<sup>-/-</sup> mice. Collectively, these data suggest that VU0468554 represents a promising new pharmacological tool for targeting cardiac GIRK channels with therapeutic implications for relevant cardiac arrhythmias.**

## **SIGNIFICANCE STATEMENT**

While cardiac GIRK channel inhibition shows promise for the treatment of supraventricular arrhythmias, the absence of subtype-selective channel inhibitors has hindered exploration into this therapeutic strategy. This study utilizes whole-cell patch-clamp electrophysiology to characterize the new GIRK channel inhibitor VU0468554 in HEK cells and primary cultures. We report that VU0468554 exhibits a favorable pharmacodynamic profile for cardiac over neuronal GIRK channels and partially reverses GIRK-mediated bradycardia in the isolated mouse heart model.

## INTRODUCTION

G protein-gated inwardly rectifying K<sup>+</sup> (GIRK/Kir3) channels are critical mediators of cell excitability in the heart and brain (Luscher and Slesinger, 2010; Slesinger and Wickman, 2015). In the heart, GIRK channels are heterotetrameric complexes made up of GIRK1 and GIRK4 subunits in 1:1 stoichiometry (Corey et al., 1998; Krapivinsky et al., 1995). Cardiac GIRK channels are predominantly expressed in atrial and nodal tissue, where they mediate much of the influence of the parasympathetic branch of the autonomic nervous system on cardiac physiology (Bettahi et al., 2002; Lee et al., 2018; Mesirca et al., 2013; Wickman et al., 1998). Activation of the M<sub>2</sub> muscarinic receptor (M<sub>2</sub>R) by acetylcholine released from postganglionic parasympathetic neurons triggers the Gβγ-dependent activation of GIRK channels in sinoatrial nodal (SAN) cells and atrial myocytes (Lee et al., 2018; Logothetis et al., 1987; Mesirca et al., 2013; Posokhova et al., 2013; Wickman et al., 1994), decreasing heart rate (HR) and increasing heart rate variability (HRV) (Lee et al., 2018; Wickman et al., 1998). Cardiac GIRK channel activation also shortens action potential duration (APD) and effective refractory period (ERP) (Wang et al., 2013b).

Increased GIRK channel activity in atrial and nodal tissue has been implicated in the pathophysiology of nodal and atrial rhythm disorders. A mutation in GNB2, which encodes Gβ2 and results in exaggerated GIRK-dependent signaling, has been identified in human patients with familial sinus node dysfunction (Long et al., 2020; Stallmeyer et al., 2017). Furthermore, increased GIRK channel activity has been noted in patients suffering from chronic atrial fibrillation (AF) (Dobrev et al., 2005; Voigt et al., 2007). Indeed, a study using a combination of optical mapping and immunoblotting revealed that re-entry drivers for adenosine-induced AF were localized to areas with co-expression of GIRK4 and the A<sub>1</sub> adenosine receptor (A<sub>1</sub>R) in human atria (Li et al., 2016). Similar observations have been reported in the mouse, where

genetic ablation of a negative regulator of GIRK-dependent signaling, Regulator of G protein Signaling 6 (RGS6), increased susceptibility to pacing-induced AF (Posokhova et al., 2013; Posokhova et al., 2010).

Pharmacological inhibition and genetic ablation of GIRK channels have been shown to rescue and/or terminate supraventricular arrhythmias such as AF and nodal dysfunction. The bee venom peptide tertiapin, a selective blocker of GIRK channels, terminates pharmacologically and vagally induced AF in canines (Hashimoto et al., 2006). Conversely, mice lacking cardiac GIRK channels are resistant to both pacing-induced AF and arrhythmias induced by vagus nerve stimulation (Kovoor et al., 2001; Lee et al., 2018). Additionally, genetic ablation of *Girk4* rescues symptoms of sick sinus syndrome and atrioventricular (AV) block in mouse models of nodal dysfunction (Mesirca et al., 2014; Mesirca et al., 2016). Intriguingly, while loss K<sup>+</sup> channel activity is normally associated with an increase in ventricular arrhythmia susceptibility (Ramalho and Freitas, 2018; Vandenberg et al., 2012), ablation of GIRK channels in ventricular tissue does not increase susceptibility to ventricular arrhythmia (Anderson et al., 2018). Collectively, these studies suggest that inhibition of cardiac GIRK channels may represent a safe therapeutic intervention for the treatment of certain types of cardiac rhythm disorders.

While the lack of pharmacological tools has impeded progress on assessing the therapeutic potential of targeting cardiac GIRK channels to treat cardiac rhythm disorders, small molecule modulators of GIRK channels have been recently identified (Cui et al., 2021; Kaufmann et al., 2013; Wen et al., 2013; Xu et al., 2020; Zhao et al., 2020). This group includes ML297, a selective activator of GIRK1-containing GIRK channels that exhibits a modest preference for the neuronal (GIRK1/GIRK2) relative to the cardiac (GIRK1/GIRK4) GIRK channel subtype (Wydeven et al., 2014). Using ML297 as a chemical scaffold and a fluorescence-based thallium flux assay, the structural derivative VU0468554 was identified as a novel GIRK channel inhibitor

that exhibited selectivity for the cardiac (GIRK1/GIRK4) relative to the neuronal (GIRK1/GIRK2) GIRK channel subtype (Wen et al., 2013). Here, we probe the selectivity and mechanisms of VU0468554 inhibition of recombinant and native GIRK channels. Our work suggests that VU0468554 is a promising GIRK1/GIRK4-selective inhibitor that could serve as a lead compound for the development of new potential therapeutics for treating cardiac arrhythmias.

## MATERIALS and METHODS

**Animals.** Animal experiments were approved by the Institutional Animal Care and Use Committee at the University of Minnesota. Both inbred and purchased (Jackson Laboratory, Bar Harbor, ME) male and female C57BL/6J mice were used for whole-cell electrophysiology and isolated heart studies. Generation of *Girk1*<sup>-/-</sup>, *Girk2*<sup>-/-</sup>, and *Girk4*<sup>-/-</sup> mice was described previously (Bettahi et al., 2002; Signorini et al., 1997; Wickman et al., 1998).

**HEK cell culture and transfection.** HEK293T cells (ATCC; Manassas, VA) were maintained at 37°C and 5% CO<sub>2</sub> in DMEM containing 10% (vol/vol) FBS, 1% sodium pyruvate, 1% glutamax, and 1% antibiotic-antimycotic (Gibco; Thermo Fisher Scientific, Inc., Waltham, MA). Cells were dislodged with Trypsin-EDTA solution (MilliporeSigma; Burlington, MA) at 70-90% confluency and plated onto 8-mm glass coverslips. After at least 1 h after plating, cells were transfected with pcDNA3-based expression constructs in the following 2 groups by calcium phosphate technique: Group 1: M<sub>2</sub>R (50 ng/coverslip), GIRK1-AU5 (50 ng/coverslip), GIRK4-AU5 (50 ng/coverslip), eGFP (20 ng/coverslip); Group 2: M<sub>2</sub>R (50 ng/coverslip), GIRK1-AU5 (50 ng/coverslip), GIRK2-myc (50 ng/coverslip), eGFP (20 ng/coverslip). Experiments were conducted 18-36 h after transfection.

**SAN cell culture.** SAN cells were isolated from young adult (2-3 months) mice (male and female) as described (Anderson et al., 2018; Anderson et al., 2020). In brief, mice were anesthetized with ketamine (100 mg/kg) and xylazine (10 mg/kg) and hearts were excised into Tyrode's solution (in mM): 140 NaCl, 5.4 KCl, 1.2 KH<sub>2</sub>PO<sub>4</sub>, 1.0 MgCl<sub>2</sub>, 1.8 CaCl<sub>2</sub>, 5.55 glucose, 5 HEPES (pH 7.4 with NaOH). SAN tissue was then excised and placed into a modified Tyrode's solution containing (in mM): 140 NaCl, 5.4 KCl, 1.2 KH<sub>2</sub>PO<sub>4</sub>, 0.2 CaCl<sub>2</sub>, 50 taurine, 18.5 glucose, 5 HEPES, 0.1% BSA (pH 6.9 with NaOH), with elastase (0.3 mg/mL, Worthington



Biochemical Corp., Lakewood, NJ) and collagenase II (0.21 mg/mL; Sigma Aldrich, St. Louis, MO) for 30 min at 37°C. SAN tissue was then washed in a solution containing (in mM): 100 L-glutamic acid/potassium salt, 10 L-aspartic acid/potassium salt, 25 KCl, 10 KH<sub>2</sub>PO<sub>4</sub>, 2 MgSO<sub>4</sub>, 20 taurine, 5 creatine, 0.5 EGTA, 20 glucose, 5 HEPES, 0.1% BSA (pH 7.2 with KOH) and triturated 3x before being plated onto laminin (25 µg/mL) coated glass coverslips. The cells were incubated at 37°C for 1 h before recording and used within 8 hours.

**Hippocampal neuron culture.** Primary cultures of hippocampal neurons were prepared as described (Vo et al., 2019). Briefly, extracted hippocampi from neonatal (P0–4) pups were placed into an ice-cold modified Hank's Balanced Salt Solution (MilliporeSigma) (in mM): 3 HEPES-NaOH (pH 7.1), kynurenic acid/12 Mg<sub>2</sub>SO<sub>4</sub>, and 5.5 D-glucose. The tissue was digested for 20 min with papain and DNase I at 37°C with occasional inversion. Hippocampi were mechanically dissociated in growth medium containing Neural-basal A medium, 2% B27 supplement, 0.5 mM Glutamax (MilliporeSigma), and antibiotic-antimycotic (Gibco; Thermo Fisher Scientific, Inc.) using trituration with 1 mL pipettes. Neurons were pelleted by centrifugation (150 rcf) and plated onto 8-mm glass coverslips pre-coated with poly-L-lysine in 48-well plates. Neurons were maintained in culture in a humidified 5% CO<sub>2</sub> incubator at 37°C, and half of the medium was replaced with fresh growth medium every 3-4 d. Neurons were kept in culture for 10-14 d before experimentation.

**Electrophysiology.** Electrophysiological recordings were performed as described (Vo et al., 2019). In brief, transfected HEK cells, pyramidal-shaped, hippocampal neurons (capacitances between 80 and 200 pF), or thin, striated SAN cells (capacitances between 15 and 40 pF), were transferred to a low-K<sup>+</sup> bath solution consisting of (in mM): 130 NaCl, 5.4 KCl, 1 CaCl<sub>2</sub>, 1 MgCl<sub>2</sub>, 5.5 D-glucose, and 5 HEPES/NaOH (pH 7.4). Fire-polished borosilicate patch pipettes were

filled with K-gluconate pipette solution containing (in mM): 140 K-gluconate, 2 MgCl<sub>2</sub>, 1.1 EGTA, 5 HEPES, 2 Na<sub>2</sub>-ATP, 0.3 Na-GTP, and 5 Na<sub>2</sub>-phosphocreatine (pH 7.2). Upon achieving whole-cell access, cells were held in voltage-clamp mode at -70 mV. Currents were measured in a high-K<sup>+</sup> bath solution containing (in mM): 120 NaCl, 25 KCl, 1 CaCl<sub>2</sub>, 1 MgCl<sub>2</sub>, 5.5 D-glucose, and 5 HEPES/NaOH (pH 7.4). VU0468554 and ML297 were dissolved in DMSO and then diluted with high-K<sup>+</sup> bath solution. Baclofen and carbachol (CCh) were dissolved in high-K<sup>+</sup> bath solution. Responses were measured as the difference in holding current at baseline (in High K<sup>+</sup> solution) and holding current following agonist, antagonist, or agonist/antagonist application. Maximal response and concentration-response experiments were performed on separate cells. Only experiments in which the access resistance was stable and low (<20 MΩ) were included in the analysis. The liquid-junction potential, predicted to be -17 mV using JPCalc software (Molecular Devices, LLC, Sunnyvale, CA), was not corrected.

**Isolated heart recordings.** Hearts from young adult (2-3 months) mice (male and female) were excised and placed into ice-cold, oxygenated Tyrode's solution and the aorta was quickly cannulated. Cannulated hearts were then placed into a warm (37±1°C) Tyrode's bath, and platinum recording electrodes (iWorx; Dover, NH) were placed on or near the surface of the heart. Oxygenated Tyrode's solution was then perfused at 2-3 mL/min and a baseline HR was recorded for 10 min. After the baseline HR was acquired, 1 μM CCh was perfused and allowed to stabilize for 15 min. While CCh was still being perfused, a bolus injection of either vehicle (1:100 DMSO) or VU0468554 (10 μM) was injected through a port in the Langendorf apparatus. The ECG signal was acquired with LabScribe v.3 software (iWorx) and filtered as appropriate. The derivative of the signal was computed to account for movements in baseline and to amplify the signal for subsequent analysis. A 15 s segment from each time point (baseline, CCh 5 min

post, 10 min post) was then exported to Kubios HRV v.2 for HR analysis, utilizing artifact correction as appropriate.

**Statistical analysis.** The experiments included in this study were done in an exploratory manner and not done according to a preset plan. All data were analyzed using Prism v.8.2.1 software (GraphPad Software; San Diego, CA) and are presented as mean  $\pm$  SD. The level of statistical significance was set at  $P < 0.05$ .  $IC_{50}$  and  $EC_{50}$  values were calculated from data plotted as  $\log(\text{inhibitor})/\log(\text{agonist})$  vs. response with nonlinear regression, variable slope models that did not assume standard slopes, with the following curve-fitting equations:

$$Y = \text{Bottom} + (\text{Top} - \text{Bottom}) / (1 + 10^{((\text{Log}IC_{50} - X) * \text{HillSlope})})$$

$$Y = \text{Bottom} + (\text{Top} - \text{Bottom}) / (1 + 10^{((\text{Log}EC_{50} - X) * \text{HillSlope})})$$

Specific statistical tests used for data analysis are denoted within the figure legends.

## RESULTS

We first investigated the inhibitory actions of VU0468554 (**Fig. 1A**) with whole-cell patch-clamp electrophysiology in HEK cells transfected with either GIRK1/GIRK4 or GIRK1/GIRK2 channel subtypes. Whole-cell GIRK channel activity was measured in transfected HEK cells, in a high-K<sup>+</sup> bath solution at a holding potential of -70 mV. Under these conditions, application of VU0468554 (10 μM) inhibited basal GIRK channel activity (*i.e.*, increased holding current) in HEK cells expressing either channel subtype (**Fig. 1B**); the increase was slightly, but not significantly, larger in cells expressing GIRK1/GIRK4 channels as compared to GIRK1/GIRK2-expressing cells (**Fig. 1C**). We also co-expressed M<sub>2</sub>R with GIRK1/GIRK4 or GIRK1/GIRK2 in HEK cells to assess the ability of VU0468554 to inhibit receptor-induced GIRK channel activity. The non-selective muscarinic receptor agonist carbachol (CCh, 10 μM) evoked reliable inward currents in both GIRK1/GIRK4- and GIRK1/GIRK2-expressing HEK cells (**Fig. 1B**). VU0468554 blocked a significantly larger fraction of the CCh-induced current in cells expressing GIRK1/GIRK4 as compared to GIRK1/GIRK2 channels (**Fig. 1D**), but no difference in VU0468554 potency (IC<sub>50</sub>) was detected between GIRK channel subtypes (**Fig. 1E,F**). Reversal of CCh-induced currents past baseline in GIRK1/GIRK4-expressing HEK cells likely reflects the combined inhibition of basal (**Fig. 1C**) and agonist-induced (**Fig. 1D**) GIRK channel activity.

We also examined the impact of VU0468554 on GIRK channel activity in native cell types. Consistent with published reports (Lee et al., 2018; Posokhova et al., 2013), CCh (10 μM) elicited inward currents in SAN cells from wild-type but not *Girk4*<sup>-/-</sup> mice (**Fig. 2A**). Previously, we demonstrated that CCh-induced currents in wild-type SAN cells were reversed by application of tertiapin-Q (Anderson et al., 2020). VU0468554 reversed CCh-induced GIRK currents in SAN cells in a dose-dependent manner, inhibiting approximately 73% of the CCh-induced response at the highest dose tested (10 μM; **Fig. 2A-C**). VU0468554 is a synthetic derivative of ML297,

which selectively activates GIRK1-containing GIRK channels (Wydeven et al., 2014). VU0468554 (10  $\mu$ M) reversibly increased the holding current of SAN cells from wild-type mice, likely due to inhibition of basal GIRK channel activity as this effect was absent in SAN cells from *Girk1*<sup>-/-</sup> mice (**Fig. 2D,E**). Thus, under these recording conditions, VU0468554 is selective for GIRK1-containing GIRK channels present in SAN cells.

Cultured hippocampal neurons from wild-type mice exhibit a GIRK conductance mediated by GIRK1/GIRK2 channels (Wydeven et al., 2014; Wydeven et al., 2012). Indeed, the selective GABA<sub>B</sub> receptor agonist baclofen (100  $\mu$ M) elicited reliable inward currents in hippocampal neurons from C57BL/6J mice that were absent in neurons from *Girk2*<sup>-/-</sup> mice (**Fig. 2A**). VU0468554 dose-dependently inhibited baclofen-induced currents in hippocampal neurons, but the maximal inhibition observed was only 20% of the baclofen-induced response (**Fig. 2A-C**), significantly smaller than the fractional inhibition of receptor-induced cardiac GIRK response in SAN cells (**Fig. 2B**). Thus, VU0468554 is a more effective inhibitor of cardiac GIRK channels than neuronal GIRK channel subtypes, as assessed in both heterologous expression and primary culture models.

To further investigate the mechanism of inhibition exhibited by VU0468554 on the cardiac GIRK channel, we examined the impact of a maximally effective dose of VU0468554 (10  $\mu$ M) on the efficacy (maximal response) and potency (EC<sub>50</sub>) of CCh (**Fig. 3A-C**). VU0468554 decreased the maximal response induced by CCh, and this effect was not overcome by higher concentrations of CCh (**Fig. 3C**), suggesting that VU0468554 inhibits receptor-induced GIRK channel activity in a non-competitive manner. We also observed a slight, yet significant decrease in CCh potency, as evidenced by an increase in the EC<sub>50</sub> of CCh-induced responses (**Fig. 3B**). This suggests that the inhibition of CCh-induced GIRK channel responses may be un-competitive, where

inhibition is affected by the interaction between the GIRK channel and  $G\beta\gamma$ , instead of solely non-competitive.

We next examined the VU0468554-dependent inhibition of cardiac GIRK channel activity evoked by ML297, which activates GIRK channels in a G protein-independent manner, presumably via direct binding (Wydeven et al., 2014) (**Fig. 3D**). Addition of VU0468554 (10  $\mu$ M) decreased the apparent potency of ML297 (**Fig. 3E**), consistent with competitive inhibition of ML297. While we also noted a modest VU0468554-dependent decrease in the efficacy of ML297 (**Fig. 3F**), the diminished amplitude of ML297-induced responses in the presence of VU0468554 likely reflects an inability to test higher concentrations of ML297 due to limited aqueous solubility of this compound.

Lastly, we investigated whether VU0468554 blocked the bradycardic effect of muscarinic receptor activation. We obtained baseline heart rate (HR) from isolated wild-type and *Girk4*<sup>-/-</sup> mouse hearts, and then perfused hearts with CCh (1  $\mu$ M). As expected, the decrease in HR upon perfusion of CCh was significantly blunted in hearts from *Girk4*<sup>-/-</sup> mice (**Fig. 4B**). After stabilization of the CCh-induced reduction in HR, we applied a bolus of VU0468554 (10  $\mu$ M) or vehicle (1:100 DMSO). In wild-type mice, vehicle administration did not reverse the CCh-induced bradycardia (**Fig. 4**), as assessed at 5 and 10-min post-injection timepoints. In contrast, VU0468554 partially reversed (~20%) CCh-induced bradycardia at 5 min and 10 min post-injection (**Fig. 4A-C**). This effect was not observed on the residual CCh-induced bradycardia in isolated hearts from *Girk4*<sup>-/-</sup> mice, indicating that the impact of VU0468554 is likely due to the selective inhibition of GIRK channels (**Fig. 4B**).

## DISCUSSION

In this study, we characterized a novel cardiac GIRK channel inhibitor (VU0468554) identified in a structure-activity investigation of the GIRK channel activator ML297 (Wen et al., 2013). Our data, obtained in electrophysiological assessments of recombinant and native GIRK channels, show that VU0468554 preferentially inhibits the cardiac (GIRK1/GIRK4) compared to the neuronal (GIRK1/GIRK2) GIRK channel subtype. Moreover, we show in an isolated heart model that VU0468554 can partially reverse the bradycardic influence of muscarinic receptor activation.

The initial characterization of VU0468554 was conducted in transfected HEK cells and utilized a fluorescence-based thallium flux assay (Wen et al., 2013). In this assay, VU0468554 suppressed the basal activity of GIRK1/GIRK2 and GIRK1/GIRK4 channel subtypes and exhibited a 3-fold increased potency as an inhibitor of GIRK1/GIRK4 ( $IC_{50}$ : 0.85  $\mu$ M) relative to GIRK1/GIRK2 ( $IC_{50}$ : 2.6  $\mu$ M) channels. Using whole-cell electrophysiological assessments, we did not detect a significant channel subtype-dependent difference in VU0468554 potency in the inhibition of  $M_2$ R-activated responses. We did, however, detect a difference in the magnitude of inhibition of maximal CCh-induced responses between GIRK channel subtypes expressed in HEK cells. Indeed, VU0468554 blocked nearly all of the  $M_2$ R-induced response in HEK cells expressing GIRK1/GIRK4 channels, but only about 50% of the response in GIRK1/GIRK2-expressing cells. Similar observations were made in primary cultures of SAN cells and hippocampal neurons, with VU0468554 exhibiting a significantly stronger blockade of receptor-induced GIRK currents in SAN cells (~70%) as compared to neurons (20%). The apparent discrepancies in relative VU0468554 potency for GIRK1/GIRK2 and GIRK1/GIRK4 channel subtypes measured using thallium flux and whole-cell recording assays could be attributable to differences between inhibition of basal activity versus GPCR-activated GIRK channel activity.

VU0468554 is structurally related to ML297, a direct  $G\beta\gamma$ -independent activator of GIRK1-containing GIRK channels (Kaufmann et al., 2013; Wydeven et al., 2014). The initial structure-activity investigation involving VU0468554 and related compounds showed that they did not act on GIRK1-lacking GIRK channels (Wen et al., 2013). Site-directed mutagenesis revealed two GIRK1 residues, one in the pore helix and the other in the second membrane-spanning domain, that are necessary for the ML297-induced activation of GIRK1-containing GIRK channels (Wydeven et al., 2014). Here, we showed that VU0468554 did not impact on holding current in recordings in SAN cells from *Girk1*<sup>-/-</sup> mice (**Fig. 2D,E**). While this finding supports the contention that VU0468554 is a selective inhibitor of GIRK1-lacking GIRK channels, further investigation of the impact of VU0468554 on this sub-category of GIRK channels is warranted.

VU0468544 provoked a rightward shift in the ML297 concentration-response relationship for GIRK channel activation in SAN cells, as expected for a competitive inhibitor. We also observed a significant reduction in the amplitude of CCh-induced responses, as expected for a non-competitive inhibitor of  $G\beta\gamma$ -dependent GIRK channel activation. Surprisingly, however, we also observed a significant reduction in CCh potency in the presence of VU0468554, suggesting that VU0468554 exhibits un-competitive inhibition, where inhibition is dependent on the formation of a substrate-bound complex (Ring et al., 2014). This phenomenon could be explained if the binding of GIRK channel to  $G\beta\gamma$  is required for its inhibition by VU0468554. Indeed, some of the basal GIRK channel activity measured in heterologous systems and native cell types is  $G\beta\gamma$ -dependent (Rishal et al., 2005; Rubinstein et al., 2007). Therefore, it is possible that VU0468554 inhibition of basal GIRK channel activity by VU0468554 may depend on the formation of a GIRK: $G\beta\gamma$  complex.



Previous work has explored the potential of GIRK channel inhibitors for the treatment of cardiac arrhythmias. Tertiapin, a bee venom peptide that is relatively selective for GIRK channels (Jin et al., 1999; Jin and Lu, 1999), completely reversed CCh-induced currents in SAN cells from wild-type mice (Anderson et al., 2020), and it suppressed atrial tachyarrhythmias in canines following pacing-induced cardiac remodeling (Cha et al., 2006). NIP-142, which inhibits GIRK channels at low concentrations ( $EC_{50} = 0.64 \mu\text{M}$ ) and hERG channels at substantially higher concentrations ( $EC_{50} = 44 \mu\text{M}$ ), reversed CCh- and adenosine-induced shortening of APD (Matsuda et al., 2006), and was shown to terminate and prevent re-initiation of AF and atrial flutter in atrial canine preparations (Nagasawa et al., 2002). Here, we show that while VU0468554 strongly inhibited CCh-induced GIRK channel activity in isolated SAN cells, it only partially reversed (15-20%) CCh-induced bradycardia in the isolated mouse heart model. This apparent discrepancy could be due to the fact that while GIRK channel activation contributes to the bradycardic effect of muscarinic receptor activation in the heart (Mesirca et al., 2013; Posokhova et al., 2013), other effectors including the cAMP-dependent  $I_f$  ("funny") current and voltage-gated  $\text{Ca}^{2+}$  channels (DiFrancesco et al., 1989; Kozasa et al., 2018; Mangoni et al., 2003), also play a role. The significantly blunted response in the *Girk4*<sup>-/-</sup> mouse, however, indicates that the contribution of other effectors under the recording conditions is small. The relatively modest inhibition of GIRK channel activity by VU0468554 in the isolated heart model likely also reflects the poor aqueous solubility of the compound and the consequent inability to test higher concentrations in this model. Indeed, we were unable to fully resuspend the compound in aqueous solutions at concentrations higher than 10  $\mu\text{M}$ .

GIRK channels are also expressed at relatively low levels in ventricular tissue (Anderson et al., 2018; Dobrzynski et al., 2002; Dobrzynski et al., 2001; Yang et al., 2010), and there is evidence that they mediate, in part, muscarinic and adenosine receptor shortening of APD and ERP (Anderson et al., 2018; Liang et al., 2014). Notably, a *GIRK4/KCNJ5* loss-of-function mutation

was identified in human LQT13, a ventricular repolarization disorder (Wang et al., 2013a; Yang et al., 2010). Recent work, however, has indicated that a loss of GIRK channel function does not appear to increase ventricular arrhythmia susceptibility (Anderson et al., 2018). Therefore, therapeutic interventions aimed at suppressing GIRK channel activity for the treatment of atrial arrhythmias could represent a safer alternative to therapies that predispose patients to ventricular dysfunction.

Given the medical significance of AF and other supraventricular arrhythmias, and the limitations of existing therapeutic approaches (Mankad and Kalahasty, 2019), it is critical to pursue multiple therapeutic avenues. VU0468554 represents a new structural class of cardiac GIRK channel inhibitor with a promising pharmacodynamic profile. Indeed, the relative selectivity of VU0468554 for cardiac GIRK channels is important because inhibition of neuronal GIRK channels could provoke seizures or have undesirable neurological effects (Lujan et al., 2014; Signorini et al., 1997). Of relevance to the potential neurological effects of GIRK channel inhibitors, the GIRK channel inhibitor BMS914392 (NTC-801) was tested in human patients with AF and did not significantly reduce AF burden. This apparent lack of therapeutic efficacy, however, was likely due to the fact that the dose employed was lowered substantially to avoid neurological side effects noted previously for this compound (Machida et al., 2010; Machida et al., 2011; Podd et al., 2016; Yamamoto et al., 2014).

In conclusion, VU0468554 represents a new structural class of GIRK channel inhibitor that holds promise as a lead compound for development of selective cardiac GIRK channel inhibitors. Next-generation agents with improved solubility could prove useful as not only a new pharmacological tool for studying GIRK channels, but also have therapeutic implications in relevant cardiac arrhythmia settings.

**ACKNOWLEDGEMENTS.** The authors would like to thank Courtney Wright for exceptional care of the mouse colony.

## **AUTHORSHIP CONTRIBUTIONS**

<i>Participated in research design:</i>	Anderson, Vo, Marron Fernandez de Velasco, and Wickman
<i>Conducted experiments:</i>	Anderson and Vo
<i>Contributed new reagents or analytic tools:</i>	Hopkins and Weaver
<i>Performed data analysis:</i>	Anderson and Vo
<i>Wrote or contributed to the writing of the manuscript:</i>	Anderson, Vo, Marron Fernandez de Velasco, Hopkins, Weaver, and Wickman

## REFERENCES

- Anderson A, Kulkarni K, Marron Fernandez de Velasco E, Carlblom N, Xia Z, Nakano A, Martemyanov KA, Tolkacheva EG and Wickman K (2018) Expression and relevance of the G protein-gated K(+) channel in the mouse ventricle. *Sci Rep* **8**(1): 1192.
- Anderson A, Masuho I, Marron Fernandez de Velasco E, Nakano A, Birnbaumer L, Martemyanov KA and Wickman K (2020) GPCR-dependent biasing of GIRK channel signaling dynamics by RGS6 in mouse sinoatrial nodal cells. *Proc Natl Acad Sci U S A* **117**(25): 14522-14531.
- Bettahi I, Marker CL, Roman MI and Wickman K (2002) Contribution of the Kir3.1 subunit to the muscarinic-gated atrial potassium channel  $I_{KACH}$ . *J Biol Chem* **277**(50): 48282-48288.
- Cha TJ, Ehrlich JR, Chartier D, Qi XY, Xiao L and Nattel S (2006) Kir3-based inward rectifier potassium current: potential role in atrial tachycardia remodeling effects on atrial repolarization and arrhythmias. *Circulation* **113**(14): 1730-1737.
- Corey S, Krapivinsky G, Krapivinsky L and Clapham DE (1998) Number and stoichiometry of subunits in the native atrial G-protein-gated K<sup>+</sup> channel,  $I_{KACH}$ . *J Biol Chem* **273**(9): 5271-5278.
- Cui M, Alhamshari Y, Cantwell L, Ei-Haou S, Eptaminitaki GC, Chang M, Abou-Assali O, Tan H, Xu K, Masotti M, Plant LD, Thakur GA, Noujaim SF, Milnes J and Logothetis DE (2021) A benzopyran with antiarrhythmic activity is an inhibitor of Kir3.1-containing potassium channels. *J Biol Chem* **296**: 100535.
- DiFrancesco D, Ducouret P and Robinson RB (1989) Muscarinic modulation of cardiac rate at low acetylcholine concentrations. *Science* **243**(4891): 669-671.
- Dobrev D, Friedrich A, Voigt N, Jost N, Wettwer E, Christ T, Knaut M and Ravens U (2005) The G protein-gated potassium current  $I(K,ACH)$  is constitutively active in patients with chronic atrial fibrillation. *Circulation* **112**(24): 3697-3706.
- Dobrzynski H, Janvier NC, Leach R, Findlay JB and Boyett MR (2002) Effects of ACh and adenosine mediated by Kir3.1 and Kir3.4 on ferret ventricular cells. *Am J Physiol Heart Circ Physiol* **283**(2): H615-630.
- Dobrzynski H, Marples DD, Musa H, Yamanushi TT, Henderson Z, Takagishi Y, Honjo H, Kodama I and Boyett MR (2001) Distribution of the muscarinic K<sup>+</sup> channel proteins Kir3.1 and Kir3.4 in the ventricle, atrium, and sinoatrial node of heart. *J Histochem Cytochem* **49**(10): 1221-1234.
- Hashimoto N, Yamashita T and Tsuruzoe N (2006) Tertiapin, a selective  $I_{KACH}$  blocker, terminates atrial fibrillation with selective atrial effective refractory period prolongation. *Pharmacol Res* **54**(2): 136-141.
- Jin W, Klem AM, Lewis JH and Lu Z (1999) Mechanisms of inward-rectifier K<sup>+</sup> channel inhibition by tertiapin-Q. *Biochemistry* **38**(43): 14294-14301.
- Jin W and Lu Z (1999) Synthesis of a stable form of tertiapin: a high-affinity inhibitor for inward-rectifier K<sup>+</sup> channels. *Biochemistry* **38**(43): 14286-14293.
- Kaufmann K, Romaine I, Days E, Pascual C, Malik A, Yang L, Zou B, Du Y, Sliwoski G, Morrison RD, Denton J, Niswender CM, Daniels JS, Sulikowski GA, Xie XS, Lindsley CW and Weaver CD (2013) ML297 (VU0456810), the first potent and selective activator of the GIRK potassium channel, displays antiepileptic properties in mice. *ACS Chem Neurosci* **4**(9): 1278-1286.
- Kovoor P, Wickman K, Maguire CT, Pu W, Gehrman J, Berul CI and Clapham DE (2001) Evaluation of the role of  $I(KACH)$  in atrial fibrillation using a mouse knockout model. *J Am Coll Cardiol* **37**(8): 2136-2143.
- Kozasa Y, Nakashima N, Ito M, Ishikawa T, Kimoto H, Ushijima K, Makita N and Takano M (2018) HCN4 pacemaker channels attenuate the parasympathetic response and stabilize the spontaneous firing of the sinoatrial node. *J Physiol* **596**(5): 809-825.

- Krapivinsky G, Gordon EA, Wickman K, Velimirovic B, Krapivinsky L and Clapham DE (1995) The G-protein-gated atrial K<sup>+</sup> channel I<sub>KACH</sub> is a heteromultimer of two inwardly rectifying K(+)-channel proteins. *Nature* **374**(6518): 135-141.
- Lee SW, Anderson A, Guzman PA, Nakano A, Tolkacheva EG and Wickman K (2018) Atrial GIRK Channels Mediate the Effects of Vagus Nerve Stimulation on Heart Rate Dynamics and Arrhythmogenesis. *Front Physiol* **9**: 943.
- Li N, Csepe TA, Hansen BJ, Sul LV, Kalyanasundaram A, Zakharkin SO, Zhao J, Guha A, Van Wagoner DR, Kilic A, Mohler PJ, Janssen PM, Biesiadecki BJ, Hummel JD, Weiss R and Fedorov VV (2016) Adenosine-Induced Atrial Fibrillation: Localized Reentrant Drivers in Lateral Right Atria due to Heterogeneous Expression of Adenosine A1 Receptors and GIRK4 Subunits in the Human Heart. *Circulation* **134**(6): 486-498.
- Liang B, Nissen JD, Laursen M, Wang X, Skibsbye L, Hearing MC, Andersen MN, Rasmussen HB, Wickman K, Grunnet M, Olesen SP and Jespersen T (2014) G-protein-coupled inward rectifier potassium current contributes to ventricular repolarization. *Cardiovasc Res* **101**(1): 175-184.
- Logothetis DE, Kurachi Y, Galper J, Neer EJ and Clapham DE (1987) The beta gamma subunits of GTP-binding proteins activate the muscarinic K<sup>+</sup> channel in heart. *Nature* **325**(6102): 321-326.
- Long VP, 3rd, Bonilla IM, Baine S, Glynn P, Kumar S, Schober K, Mowrey K, Weiss R, Lee NY, Mohler PJ, Gyorke S, Hund TJ, Fedorov VV and Carnes CA (2020) Chronic heart failure increases negative chronotropic effects of adenosine in canine sinoatrial cells via A1R stimulation and GIRK-mediated IKado. *Life Sci* **240**: 117068.
- Lujan R, Marron Fernandez de Velasco E, Aguado C and Wickman K (2014) New insights into the therapeutic potential of GIRK channels. *Trends Neurosci* **37**(1): 20-29.
- Luscher C and Slesinger PA (2010) Emerging roles for G protein-gated inwardly rectifying potassium (GIRK) channels in health and disease. *Nat Rev Neurosci* **11**(5): 301-315.
- Machida T, Hashimoto N, Kuwahara I, Ogino Y, Matsuura J, Yamamoto W, Itano Y, Zamma A, Matsumoto R, Kamon J, Kobayashi T, Ishiwata N, Yamashita T, Ogura T and Nakaya H (2011) Effects of a highly selective acetylcholine-activated K<sup>+</sup> channel blocker on experimental atrial fibrillation. *Circ Arrhythm Electrophysiol* **4**(1): 94-102.
- Mangoni ME, Couette B, Bourinet E, Platzer J, Reimer D, Striessnig J and Nargeot J (2003) Functional role of L-type Cav1.3 Ca<sup>2+</sup> channels in cardiac pacemaker activity. *Proc Natl Acad Sci U S A* **100**(9): 5543-5548.
- Mankad P and Kalahasty G (2019) Antiarrhythmic Drugs: Risks and Benefits. *Med Clin North Am* **103**(5): 821-834.
- Matsuda T, Ito M, Ishimaru S, Tsuruoka N, Saito T, Iida-Tanaka N, Hashimoto N, Yamashita T, Tsuruzoe N, Tanaka H and Shigenobu K (2006) Blockade by NIP-142, an antiarrhythmic agent, of carbachol-induced atrial action potential shortening and GIRK1/4 channel. *J Pharmacol Sci* **101**(4): 303-310.
- Mesirca P, Alig J, Torrente AG, Muller JC, Marger L, Rollin A, Marquilly C, Vincent A, Dubel S, Bidaud I, Fernandez A, Seniuk A, Engeland B, Singh J, Miquerol L, Ehmke H, Eschenhagen T, Nargeot J, Wickman K, Isbrandt D and Mangoni ME (2014) Cardiac arrhythmia induced by genetic silencing of 'funny' (f) channels is rescued by GIRK4 inactivation. *Nat Commun* **5**: 4664.
- Mesirca P, Bidaud I, Briec F, Evain S, Torrente AG, Le Quang K, Leoni AL, Baudot M, Marger L, Chung You Chong A, Nargeot J, Striessnig J, Wickman K, Charpentier F and Mangoni ME (2016) G protein-gated I<sub>KACH</sub> channels as therapeutic targets for treatment of sick sinus syndrome and heart block. *Proc Natl Acad Sci U S A* **113**(7): E932-941.
- Mesirca P, Marger L, Toyoda F, Rizzetto R, Audoubert M, Dubel S, Torrente AG, Difrancesco ML, Muller JC, Leoni AL, Couette B, Nargeot J, Clapham DE, Wickman K and Mangoni ME (2013) The G-protein-gated K<sup>+</sup> channel, I<sub>KACH</sub>, is required for regulation of pacemaker activity

- and recovery of resting heart rate after sympathetic stimulation. *J Gen Physiol* **142**(2): 113-126.
- Nagasawa H, Fujiki A, Fujikura N, Matsuda T, Yamashita T and Inoue H (2002) Effects of a novel class III antiarrhythmic agent, NIP-142, on canine atrial fibrillation and flutter. *Circ J* **66**(2): 185-191.
- Podd SJ, Freemantle N, Furniss SS and Sulke N (2016) First clinical trial of specific IKACH blocker shows no reduction in atrial fibrillation burden in patients with paroxysmal atrial fibrillation: pacemaker assessment of BMS 914392 in patients with paroxysmal atrial fibrillation. *Europace* **18**(3): 340-346.
- Posokhova E, Ng D, Opel A, Masuho I, Tinker A, Biesecker LG, Wickman K and Martemyanov KA (2013) Essential Role of the m2R-RGS6-I<sub>KACH</sub> Pathway in Controlling Intrinsic Heart Rate Variability. *PLoS one* **8**(10): e76973.
- Posokhova E, Wydeven N, Allen KL, Wickman K and Martemyanov KA (2010) RGS6/Gbeta5 complex accelerates I<sub>KACH</sub> gating kinetics in atrial myocytes and modulates parasympathetic regulation of heart rate. *Circ Res* **107**(11): 1350-1354.
- Ramalho D and Freitas J (2018) Drug-induced life-threatening arrhythmias and sudden cardiac death: A clinical perspective of long QT, short QT and Brugada syndromes. *Rev Port Cardiol* **37**(5): 435-446.
- Ring B, Wrighton SA and Mohutsky M (2014) Reversible mechanisms of enzyme inhibition and resulting clinical significance. *Methods Mol Biol* **1113**: 37-56.
- Rishal I, Porozov Y, Yakubovich D, Varon D and Dascal N (2005) Gbetagamma-dependent and Gbetagamma-independent basal activity of G protein-activated K<sup>+</sup> channels. *J Biol Chem* **280**(17): 16685-16694.
- Rubinstein M, Peleg S, Berlin S, Brass D and Dascal N (2007) Galphai3 primes the G protein-activated K<sup>+</sup> channels for activation by coexpressed Gbetagamma in intact *Xenopus* oocytes. *J Physiol* **581**(Pt 1): 17-32.
- Signorini S, Liao YJ, Duncan SA, Jan LY and Stoffel M (1997) Normal cerebellar development but susceptibility to seizures in mice lacking G protein-coupled, inwardly rectifying K<sup>+</sup> channel GIRK2. *Proc Natl Acad Sci U S A* **94**(3): 923-927.
- Slesinger PA and Wickman K (2015) *Structure to function of G protein-gated inwardly rectifying (GIRK) channels*. Int Rev Neurobiol (Harris RA & Jenner P, Series Editors). Elsevier.
- Stallmeyer B, Kuss J, Kotthoff S, Zumhagen S, Vowinkel K, Rinne S, Matschke LA, Friedrich C, Schulze-Bahr E, Rust S, Seeböhm G, Decher N and Schulze-Bahr E (2017) A Mutation in the G-Protein Gene GNB2 Causes Familial Sinus Node and Atrioventricular Conduction Dysfunction. *Circ Res* **120**(10): e33-e44.
- Vandenberg JI, Perry MD, Perrin MJ, Mann SA, Ke Y and Hill AP (2012) hERG K(+) channels: structure, function, and clinical significance. *Physiol Rev* **92**(3): 1393-1478.
- Vo BN, Abney KK, Anderson A, Marron Fernandez de Velasco E, Benneyworth MA, Daniels JS, Morrison RD, Hopkins CR, Weaver CD and Wickman K (2019) VU0810464, a non-urea G protein-gated inwardly rectifying K(+) (Kir 3/GIRK) channel activator, exhibits enhanced selectivity for neuronal Kir3 channels and reduces stress-induced hyperthermia in mice. *Br J Pharmacol* **176**(13): 2238-2249.
- Voigt N, Maguy A, Yeh YH, Qi X, Ravens U, Dobrev D and Nattel S (2007) Changes in IK<sub>ACh</sub> single-channel activity with atrial tachycardia remodelling in canine atrial cardiomyocytes. *Cardiovasc Res* **77**(1): 35-43
- Wang F, Liu J, Hong L, Liang B, Graff C, Yang Y, Christiansen M, Olesen SP, Zhang L and Kanters JK (2013a) The phenotype characteristics of type 13 long QT syndrome with mutation in KCNJ5 (Kir3.4-G387R). *Heart Rhythm* **10**(10): 1500-1506.
- Wang X, Liang B, Skibsbjerg L, Olesen SP, Grunnet M and Jespersen T (2013b) GIRK channel activation via adenosine or muscarinic receptors has similar effects on rat atrial electrophysiology. *J Cardiovasc Pharmacol* **62**(2): 192-198.

- Wen W, Wu W, Romaine IM, Kaufmann K, Du Y, Sulikowski GA, Weaver CD and Lindsley CW (2013) Discovery of 'molecular switches' within a GIRK activator scaffold that afford selective GIRK inhibitors. *Bioorg Med Chem Lett* **23**(16): 4562-4566.
- Wickman K, Iniguez-Lluhl JA, Davenport PA, Taussig R, Krapivinsky GB, Linder ME, Gilman AG and Clapham DE (1994) Recombinant G-protein beta gamma-subunits activate the muscarinic-gated atrial potassium channel. *Nature* **368**(6468): 255-257.
- Wickman K, Nemec J, Gendler SJ and Clapham DE (1998) Abnormal heart rate regulation in GIRK4 knockout mice. *Neuron* **20**(1): 103-114.
- Wydeven N, Marron Fernandez de Velasco E, Du Y, Benneyworth MA, Hearing MC, Fischer RA, Thomas MJ, Weaver CD and Wickman K (2014) Mechanisms underlying the activation of G-protein-gated inwardly rectifying K<sup>+</sup> (GIRK) channels by the novel anxiolytic drug, ML297. *Proc Natl Acad Sci U S A* **111**(29): 10755-10760.
- Wydeven N, Young D, Mirkovic K and Wickman K (2012) Structural elements in the GirK1 subunit that potentiate G protein-gated potassium channel activity. *Proc Natl Acad Sci U S A* **109**(52): 21492-21497.
- Xu Y, Cantwell L, Molosh AI, Plant LD, Gazgalis D, Fitz SD, Dustrude ET, Yang Y, Kawano T, Garai S, Noujaim SF, Shekhar A, Logothetis DE and Thakur GA (2020) The small molecule GAT1508 activates brain-specific GIRK1/2 channel heteromers and facilitates conditioned fear extinction in rodents. *J Biol Chem* **295**(11): 3614-3634.
- Yamamoto W, Hashimoto N, Matsuura J, Machida T, Ogino Y, Kobayashi T, Yamanaka Y, Ishiwata N, Yamashita T, Tanimoto K, Miyoshi S, Fukuda K, Nakaya H and Ogawa S (2014) Effects of the selective K<sub>ACh</sub> channel blocker NTC-801 on atrial fibrillation in a canine model of atrial tachypacing: comparison with class Ic and III drugs. *J Cardiovasc Pharmacol* **63**(5): 421-427.
- Yang Y, Liang B, Liu J, Li J, Grunnet M, Olesen SP, Rasmussen HB, Ellinor PT, Gao L, Lin X, Li L, Wang L, Xiao J, Liu Y, Zhang S, Liang D, Peng L, Jespersen T and Chen YH (2010) Identification of a Kir3.4 mutation in congenital long QT syndrome. *Am J Hum Genet* **86**(6): 872-880.
- Zhao Y, Ung PM, Zahoranszky-Kohalmi G, Zakharov AV, Martinez NJ, Simeonov A, Glaaser IW, Rai G, Schlessinger A, Marugan JJ and Slesinger PA (2020) Identification of a G-Protein-Independent Activator of GIRK Channels. *Cell Rep* **31**(11): 107770.



## FOOTNOTES

This work was supported by the National Institutes of Health (NIH) [HL105550, DA034696, AA027544, KW]; [HL139090, AA]; [MH107399, KW, CRH, CDW]. The authors declare no conflicts of interest.

A previous version of this manuscript was included in the following PhD thesis: Anderson A (2020) Physiological contribution and molecular details of GIRK-dependent signaling in the heart. Department of Pharmacology, University of Minnesota, Minneapolis, MN (USA).

Reprint requests can be directed to Dr. Kevin Wickman (wickm002@umn.edu) at University of Minnesota, Department of Pharmacology, 6-120 Jackson Hall, 312 Church Street SE, Minneapolis, MN 55455.

## FIGURE LEGENDS

**Figure 1. VU0468554 blockade of GIRK channel subtypes expressed in HEK cells. (A)** Chemical structures of VU0468554 (top) and ML297 (bottom). **(B)** Representative traces of holding current ( $V_{\text{hold}} = -70$  mV) following application of VU0468554 (VU554, 10  $\mu\text{M}$ ) and CCh (10  $\mu\text{M}$ ) in HEK cells expressing  $M_2R$  and either GIRK1/GIRK4 (top) or GIRK1/GIRK2 channel subtypes (bottom). Scale bars: 10 s/500 pA. **(C)** Summary of the inhibition of basal GIRK channel activity by VU0468554 (10  $\mu\text{M}$ ), reported as current density, in HEK cells expressing either GIRK1/GIRK4 ( $n=7$  cells) or GIRK1/GIRK2 ( $n=9$  cells) channel subtypes ( $t_{14}=1.3$ ;  $P=0.23$ ; two-tailed unpaired  $t$ -test). **(D)** Summary of the percentage inhibition by VU0468554 (10  $\mu\text{M}$ ) of current evoked by CCh (10  $\mu\text{M}$ ) in HEK cells expressing  $M_2R$  and either GIRK1/GIRK4 ( $n=7$  cells) or GIRK1/GIRK2 ( $n=8$  cells) channel subtypes ( $t_{13}=6.7$ ; \*\*\*\* $P<0.0001$ ; two-tailed unpaired  $t$ -test). **(E)** Concentration-response curves for VU0468554-dependent inhibition of CCh-induced currents in HEK cells expressing  $M_2R$  and GIRK1/GIRK4 ( $n=11$  cells) or GIRK1/GIRK2 ( $n=9$  cells) channel subtypes. **(F)** Summary of the  $\text{Log}(IC_{50})$  extracted from concentration-response experiments examining the VU0468554-dependent inhibition of CCh-induced GIRK currents in HEK cells expressing  $M_2R$  and GIRK1/GIRK4 ( $n=11$ ) or GIRK1/GIRK2 ( $n=9$  cells) channel subtypes ( $t_6=0.9$ ;  $P=0.34$ ; two-tailed unpaired  $t$ -test).

**Figure 2. VU0468554 preferentially blocks cardiac over neuronal GIRK channels. (A)**

Representative inward currents evoked by CCh (10  $\mu$ M) in wild-type SAN cells (top left), and by baclofen (100  $\mu$ M) in wild-type hippocampal neurons (top right), and their reversal by VU0468554 (10  $\mu$ M). CCh failed to evoke currents in SAN cells from *Girk4*<sup>-/-</sup> mice, and baclofen failed to evoke responses in hippocampal neurons from *Girk2*<sup>-/-</sup> mice (bottom right). Scale bars: 10 s/500 pA. **(B)** Summary of the percentage inhibition by VU0468554 (10  $\mu$ M) of currents evoked by CCh in SAN cells (n=9 cells) or baclofen in hippocampal neurons (n=8 cells) ( $t_{15}=11.8$ ; \*\*\*\* $P<0.0001$ ; two-tailed unpaired  $t$ -test). **(C)** Summary of concentration-dependent inhibition of CCh-induced currents in SAN cells (n=10 cells) and baclofen-induced currents in hippocampal neurons from wild-type mice (n=7 cells). **(D)** Representative holding current ( $V_{\text{hold}}=-70$  mV) responses to VU0468554 (10  $\mu$ M) in SAN cells from wild-type (left) and *Girk1*<sup>-/-</sup>(right) mice. Scale bars: 5 s/100 pA. **(E)** Summary of the holding current responses evoked by VU0468554 (10  $\mu$ M) in SAN cells from wild-type (n=9) and *Girk1*<sup>-/-</sup> (n=14) mice ( $t_{21}=4.4$ ; \*\*\* $P<0.0001$ ; two-tailed unpaired  $t$ -test).

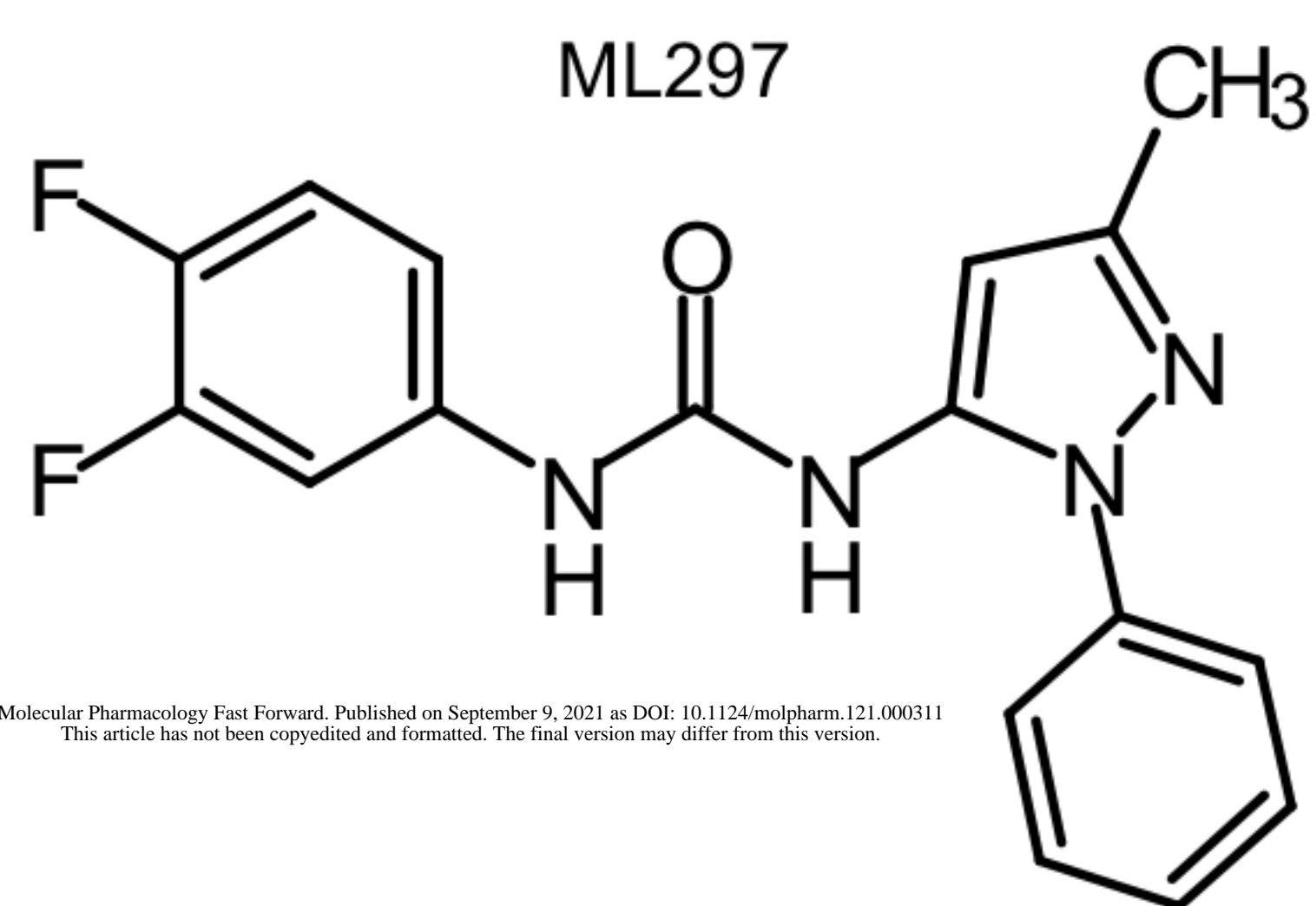
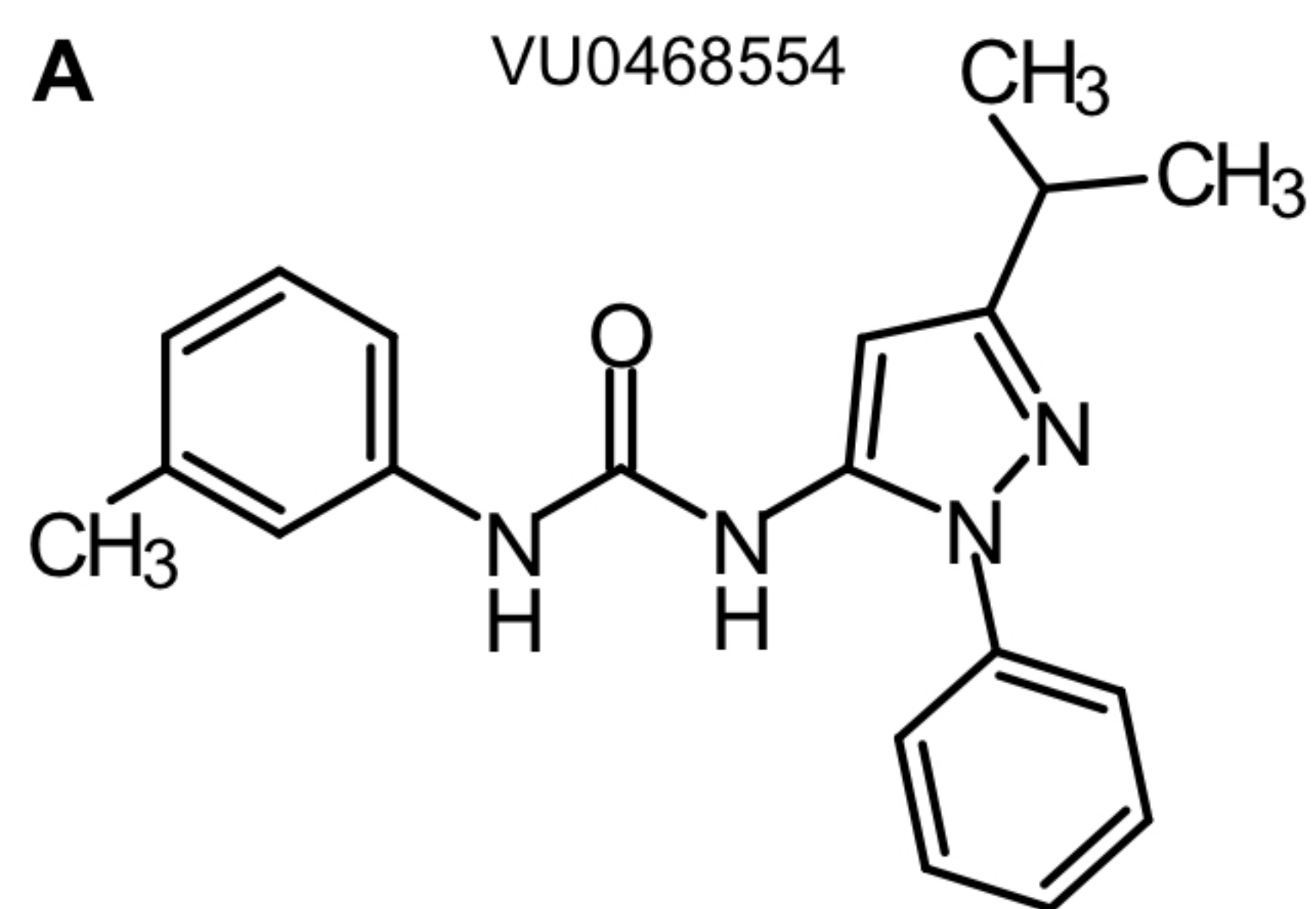
**Figure 3. Mechanism of VU0468554 inhibition of GIRK channel activity in SAN cells. (A)**

Impact of vehicle or VU0468554 (10  $\mu$ M) on the concentration-response relationship for the CCh-induced activation of GIRK channels in SAN cells. **(B)** Summary of the Log( $EC_{50}$ ) extracted from concentration-response experiments examining the impact of vehicle (n=17) or VU0468554 (10  $\mu$ M; n=11) on CCh-induced currents in wild-type SAN cells ( $t_{2,6}=2.9$ ; \* $P<0.05$ ; two-tailed unpaired  $t$ -test, Welch's correction). **(C)** Summary of maximal CCh-induced responses (current density at 100  $\mu$ M) in wild-type SAN cells in the presence (n=10 cells/3 mice) or absence (n=6 cells/1 mouse) of 10  $\mu$ M VU0468554 ( $t_{1,4}=5.4$ ; \*\*\*\* $P<0.0001$ ; two-tailed unpaired  $t$ -test). **(D)** Summary of concentration dependent experiments of ML297-induced currents in wild-type SAN cells in the presence (n=12 cells/3 mice) or absence of 10  $\mu$ M VU0468554 (n=11 cells/3 mice) **(E)** Summary of the Log( $EC_{50}$ ) extracted from concentration-response experiments examining the impact of vehicle (n=11) or VU0468554 (10  $\mu$ M; n=12) on ML297-induced currents in wild-type SAN cells ( $t_{2,1}=2.4$ ; \* $P<0.05$ ; two-tailed unpaired  $t$ -test). **(F)** Summary of maximal ML297-induced responses (current density at 100  $\mu$ M) in wild-type SAN cells in the presence (n=5 cells/1 mouse) or absence (n=6 cells/1 mouse) of 10  $\mu$ M VU0468554 ( $t_{1,4}=2.2$ ;  $P=0.06$ ; two-tailed unpaired  $t$ -test).

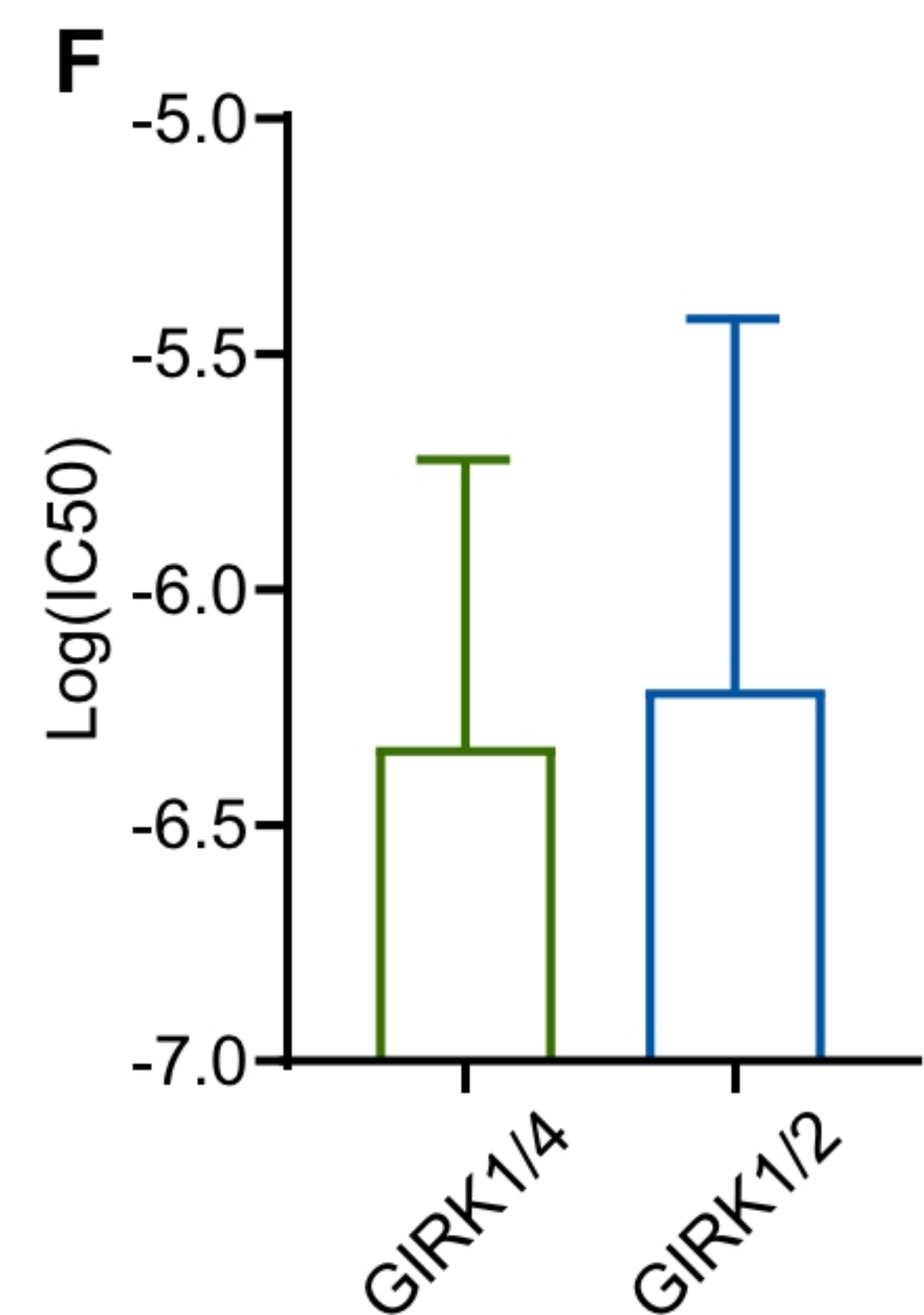
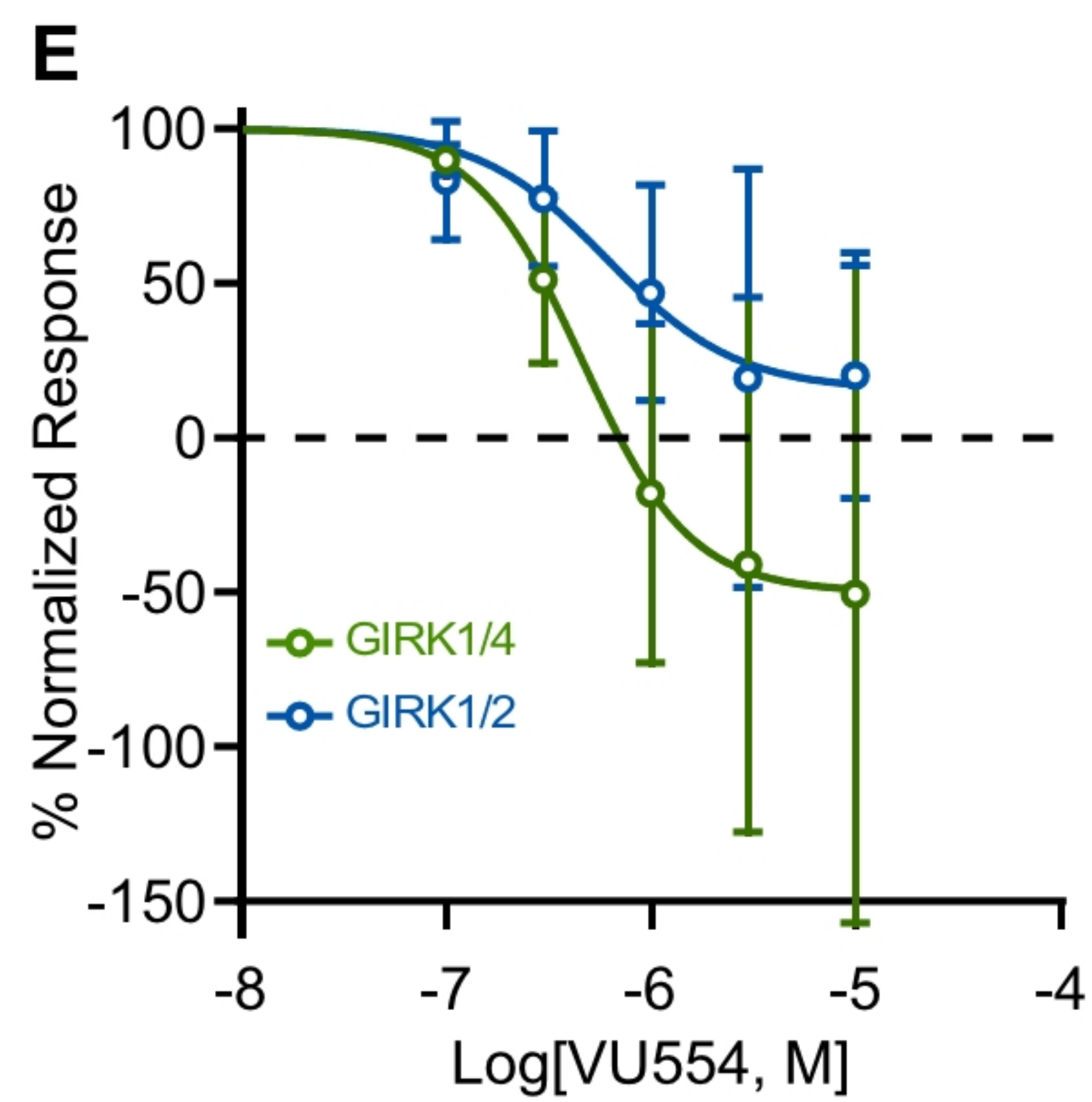
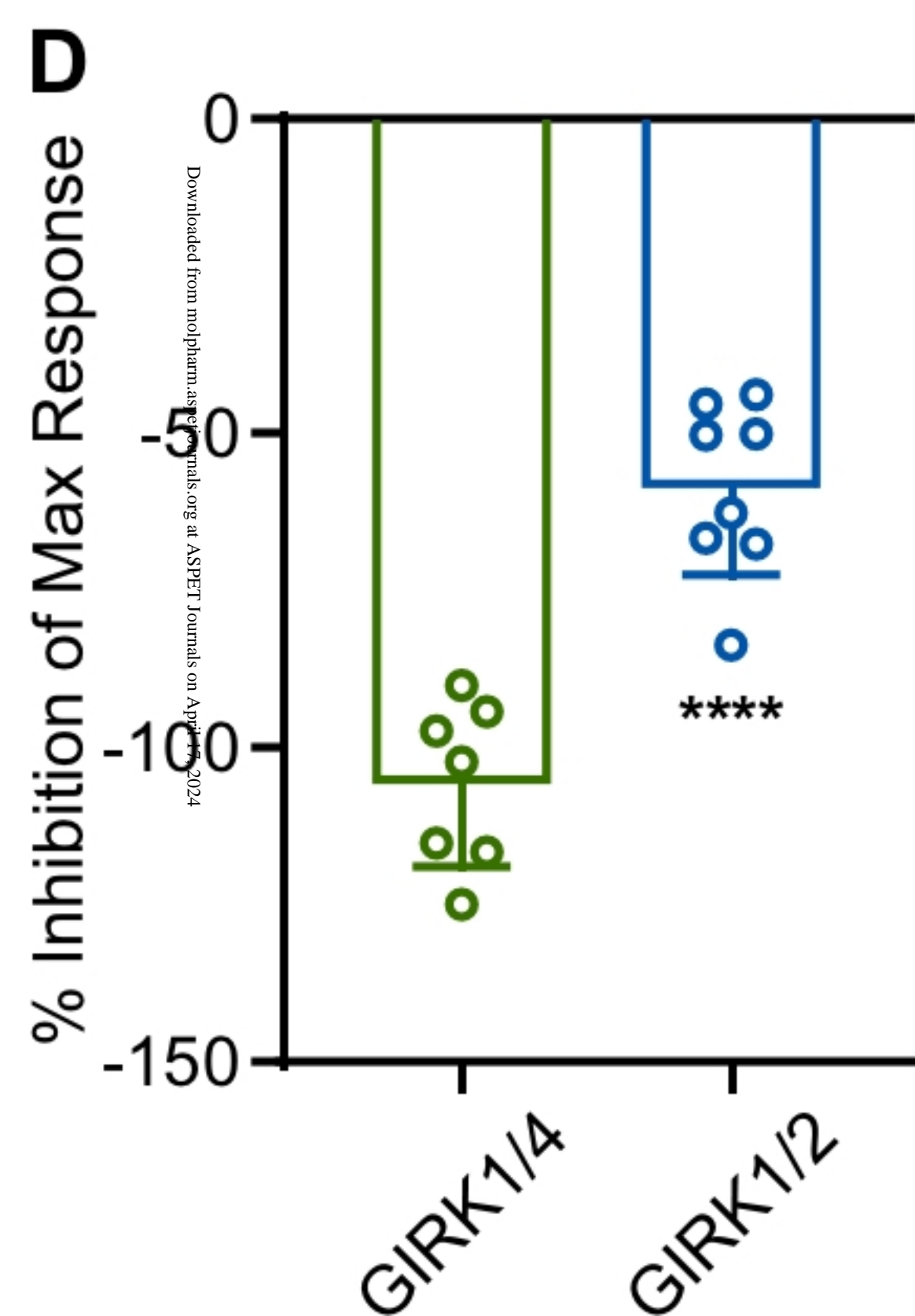
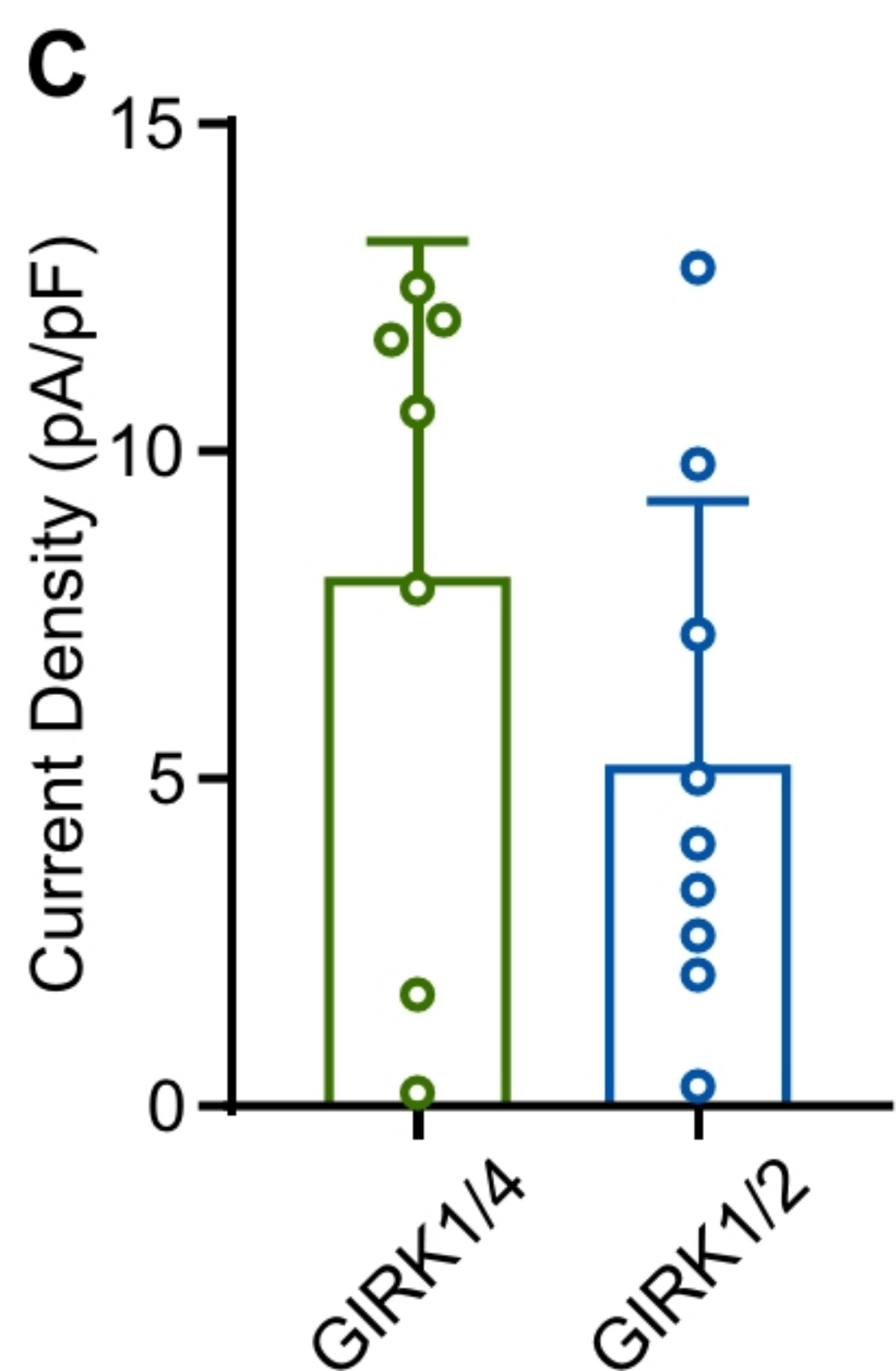
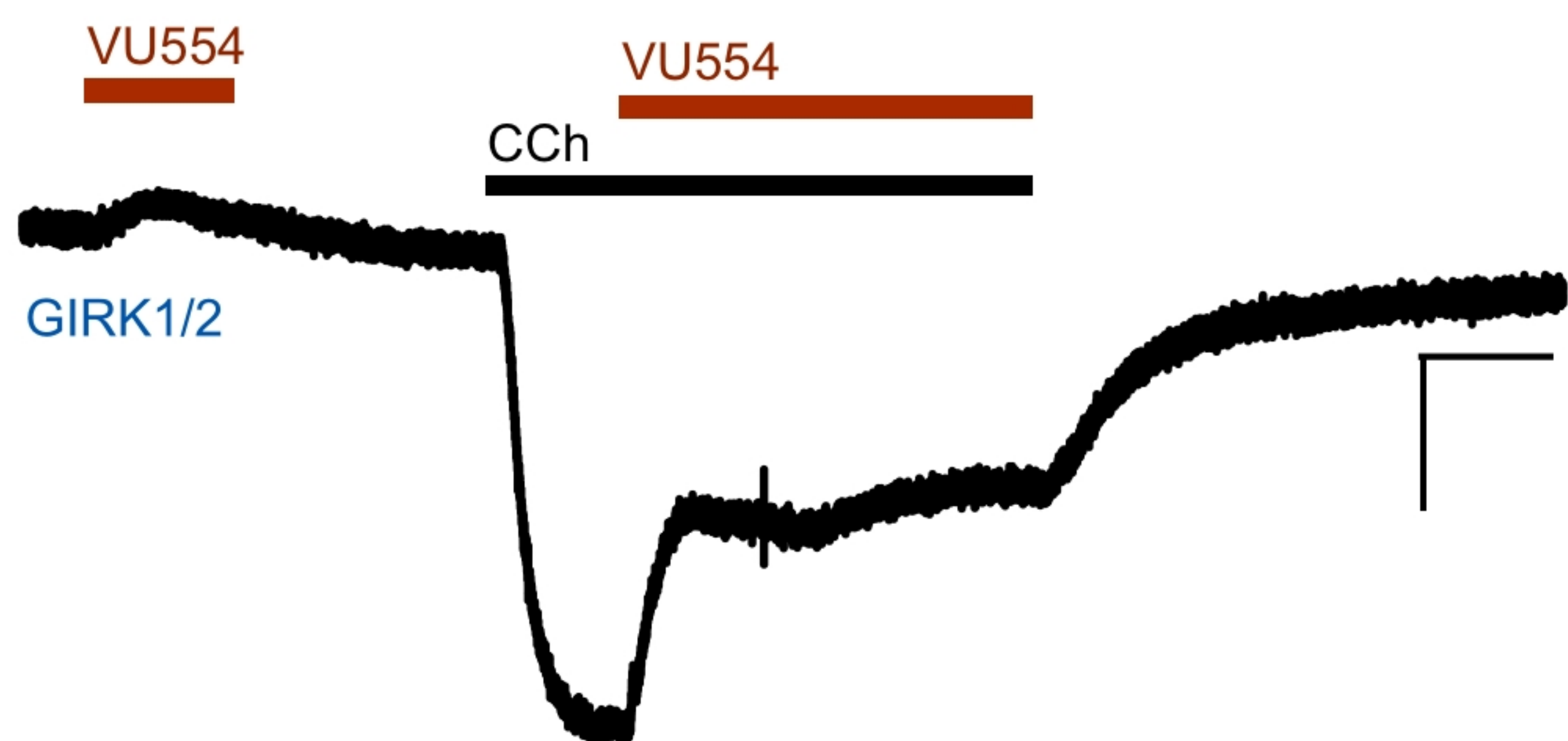
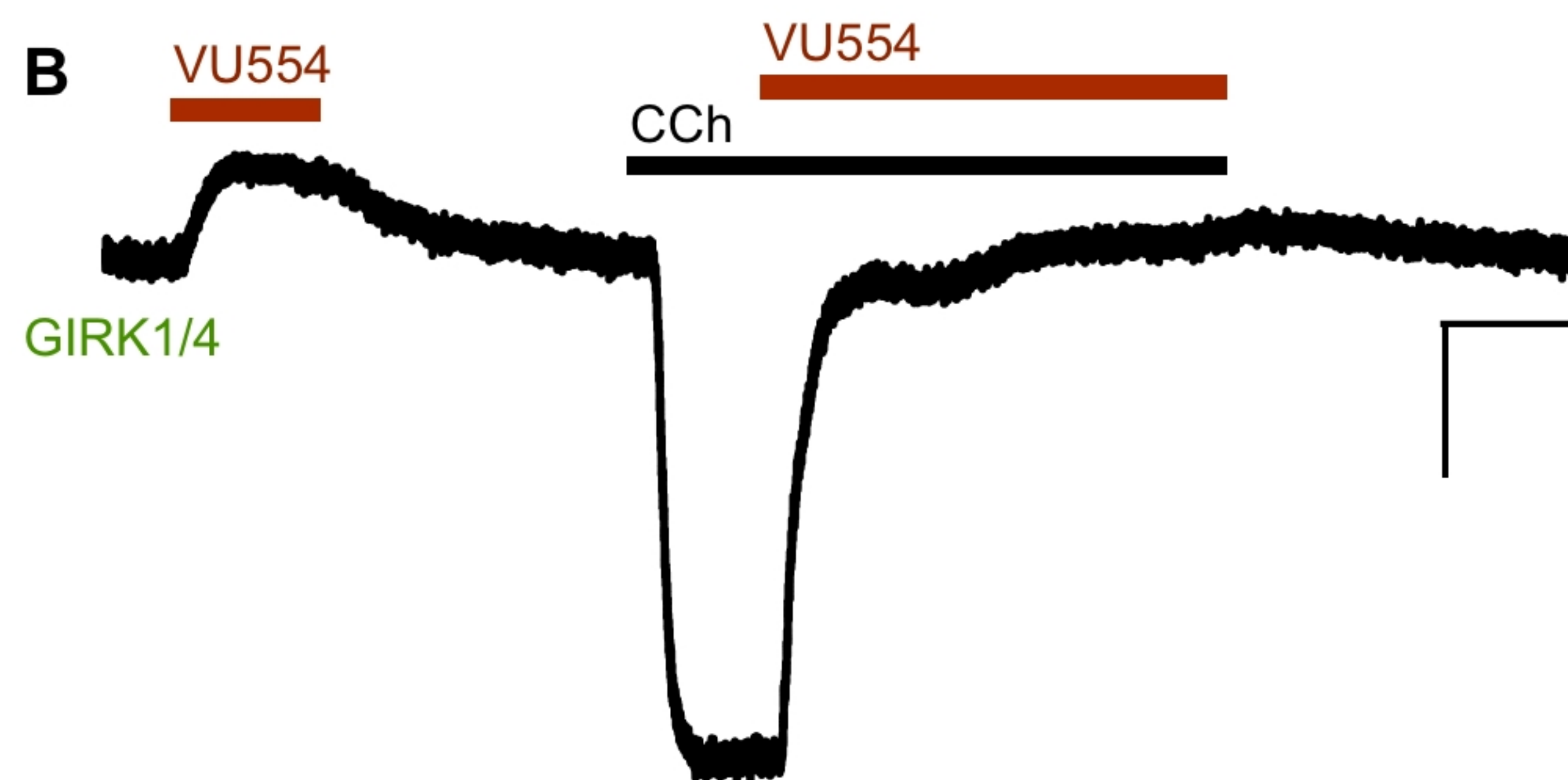
**Figure 4. VU0468554 partially reverses CCh-induced bradycardia in the isolated heart. (A)**

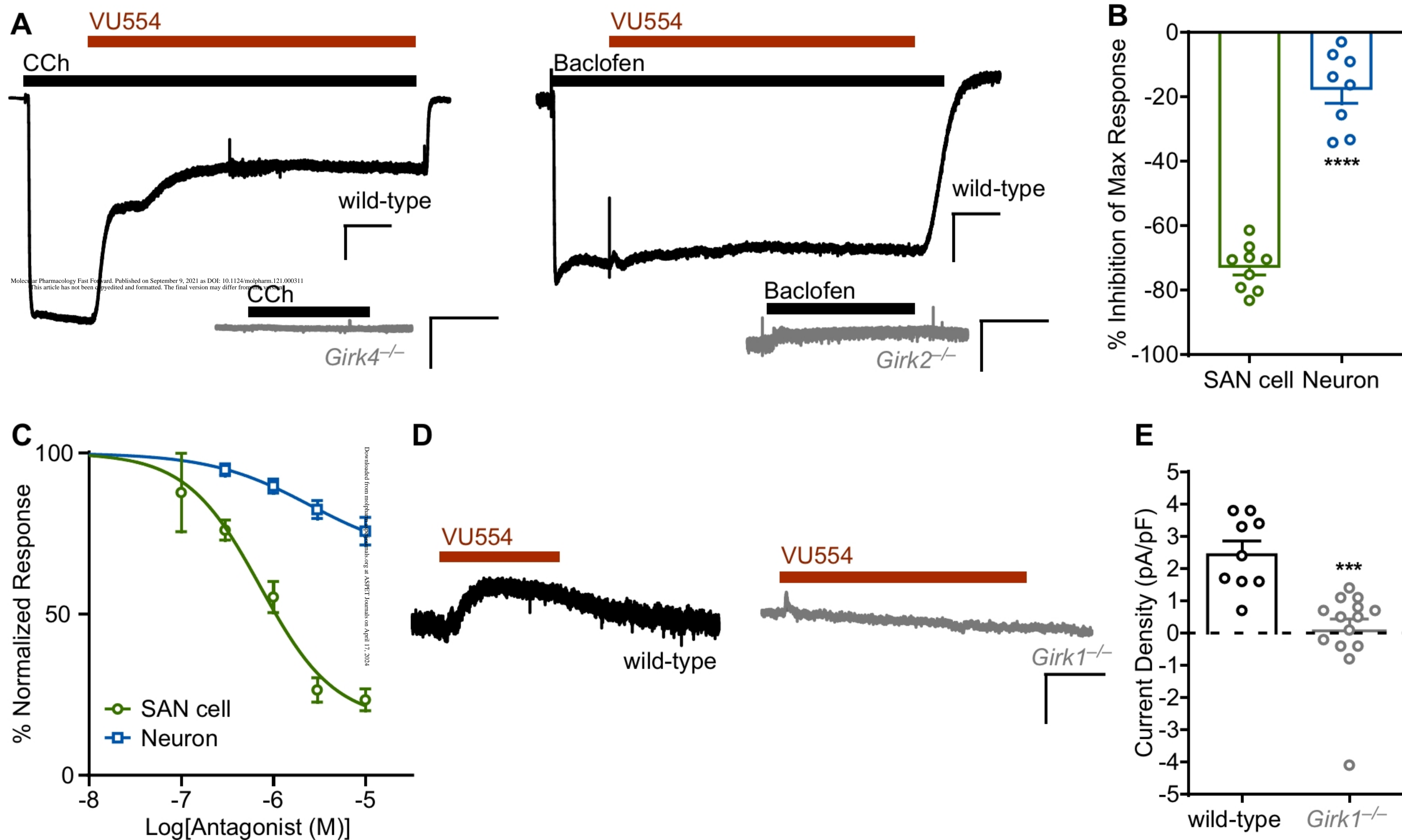
Representative isolated heart recordings from wild-type mice showing HR at baseline (left), after perfusion of CCh (10  $\mu$ M, middle), and 5 min post-injection of vehicle (1:100 DMSO, top) or VU0468554 (10  $\mu$ M, bottom) while CCh is still being perfused; scale bar: 2 s. **(B)** Summary of the percentage of baseline beating rate (% baseline beating rate = 100 - [(beating rate at timepoint on x-axis/baseline beating rate) x 100]) of isolated hearts from wild-type and *Girk4*<sup>-/-</sup> mice. There was a significant difference in the impact of CCh on hearts from wild-type (n=10) and *Girk4*<sup>-/-</sup> (n=5) mice ( $t_{15}=16.1$ , \*\*\*\* $P<0.0001$ ; two-tailed unpaired t-test). There was a significant between treatment (+/- VU554) and timepoint (CCh, 5 min post, and 10 min post) in wild-type hearts ( $F_{2,18}=11.9$ ; \*\*\* $P<0.001$ ; two-way ANOVA), with *post hoc* analysis (Bonferroni) revealing a significant difference between vehicle (n=6 hearts) and VU0468554 treatment (n=5 hearts) 10 min post-injection in wild-type hearts (\* $P<0.05$ ). There was no main effect of treatment ( $F_{1,4}=0.005$ ;  $P=0.9$ ) or timepoint ( $F_{2,8}=4.3$ ;  $P=0.1$ ), nor was there a treatment x timepoint interaction ( $F_{2,8}=0.5$ ;  $P=0.61$ ) in *Girk4*<sup>-/-</sup> mouse hearts (n=3 hearts per treatment). **(C)** Summary of the change in beating rate ( $\Delta$  beating rate = beating rate after CCh injection – beating rate measured 5 min or 10 min after vehicle/VU554 injection) of isolated hearts from wild-type mice. There was a significant effect of treatment ( $F_{1,9}=31.4$ , \*\*\* $P<0.001$ ; two-way ANOVA) but not timepoint ( $F_{1,9}=2.5$ ;  $P=0.15$ ), and no interaction between treatment and timepoint was detected ( $F_{1,9}=0.01$ ;  $P=0.92$ ).

# FIGURE 1



Molecular Pharmacology Fast Forward. Published on September 9, 2021 as DOI: 10.1124/molpharm.121.000311  
This article has not been certified by peer review and is not a certified medical product. The final version may differ from this version.



**FIGURE 2**

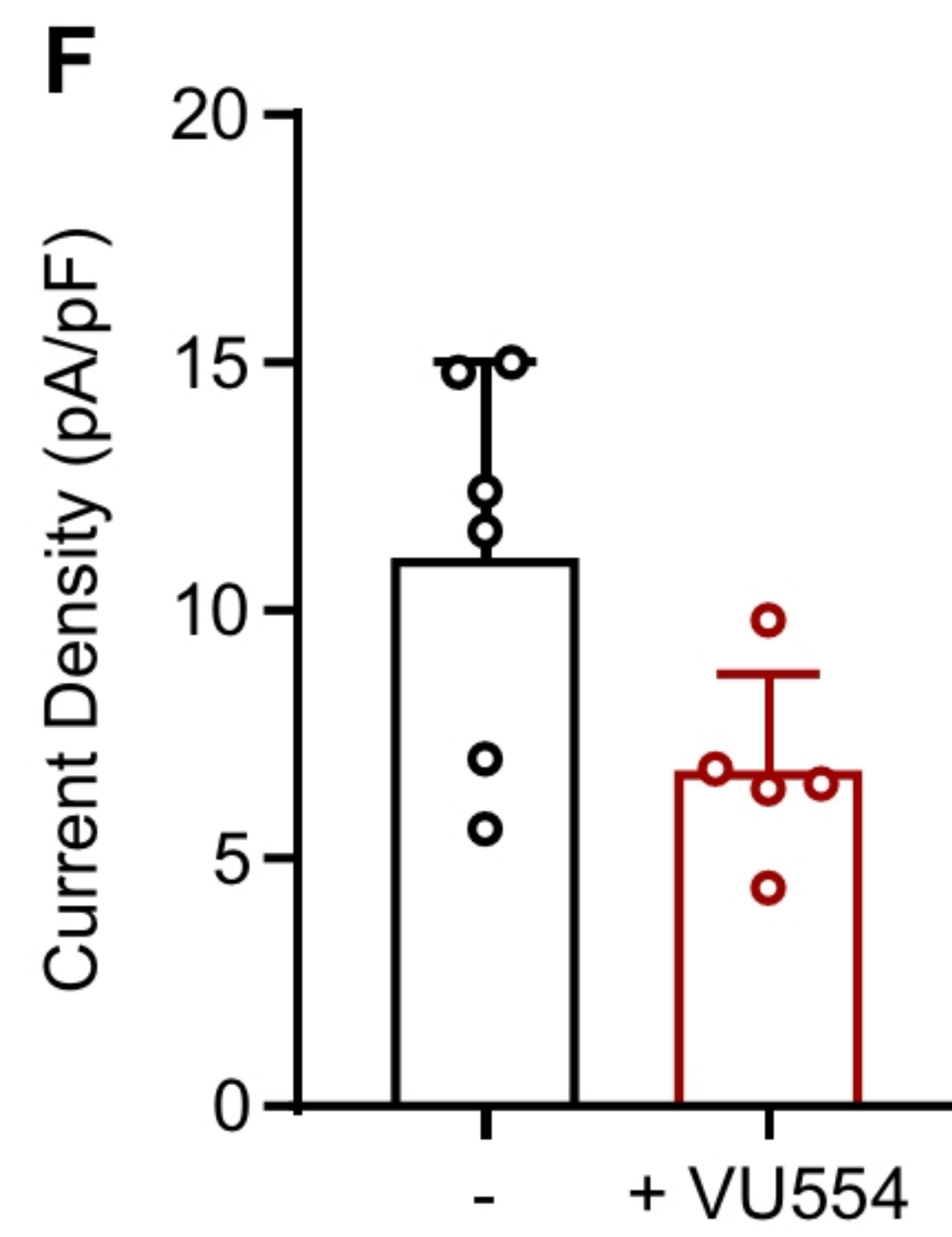
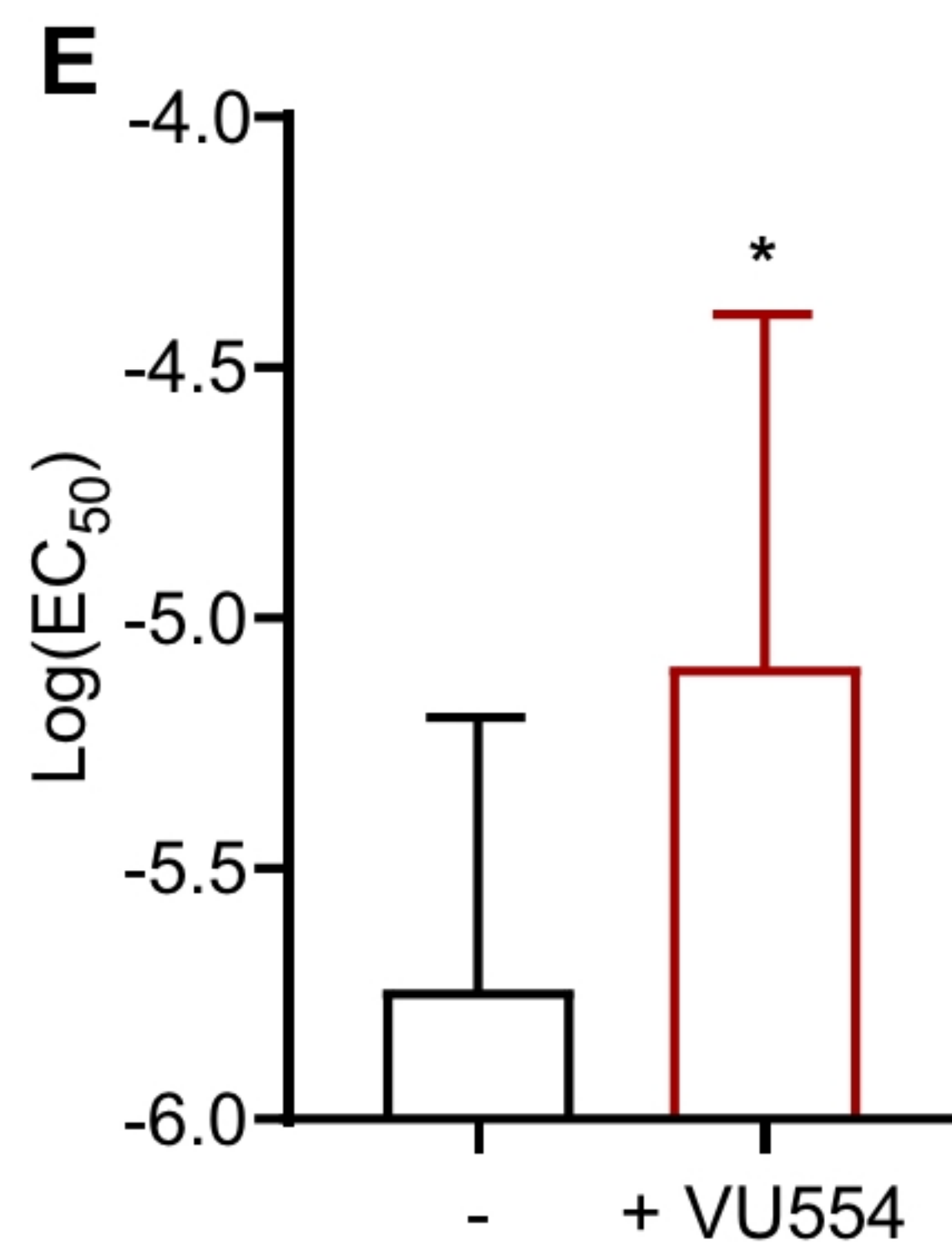
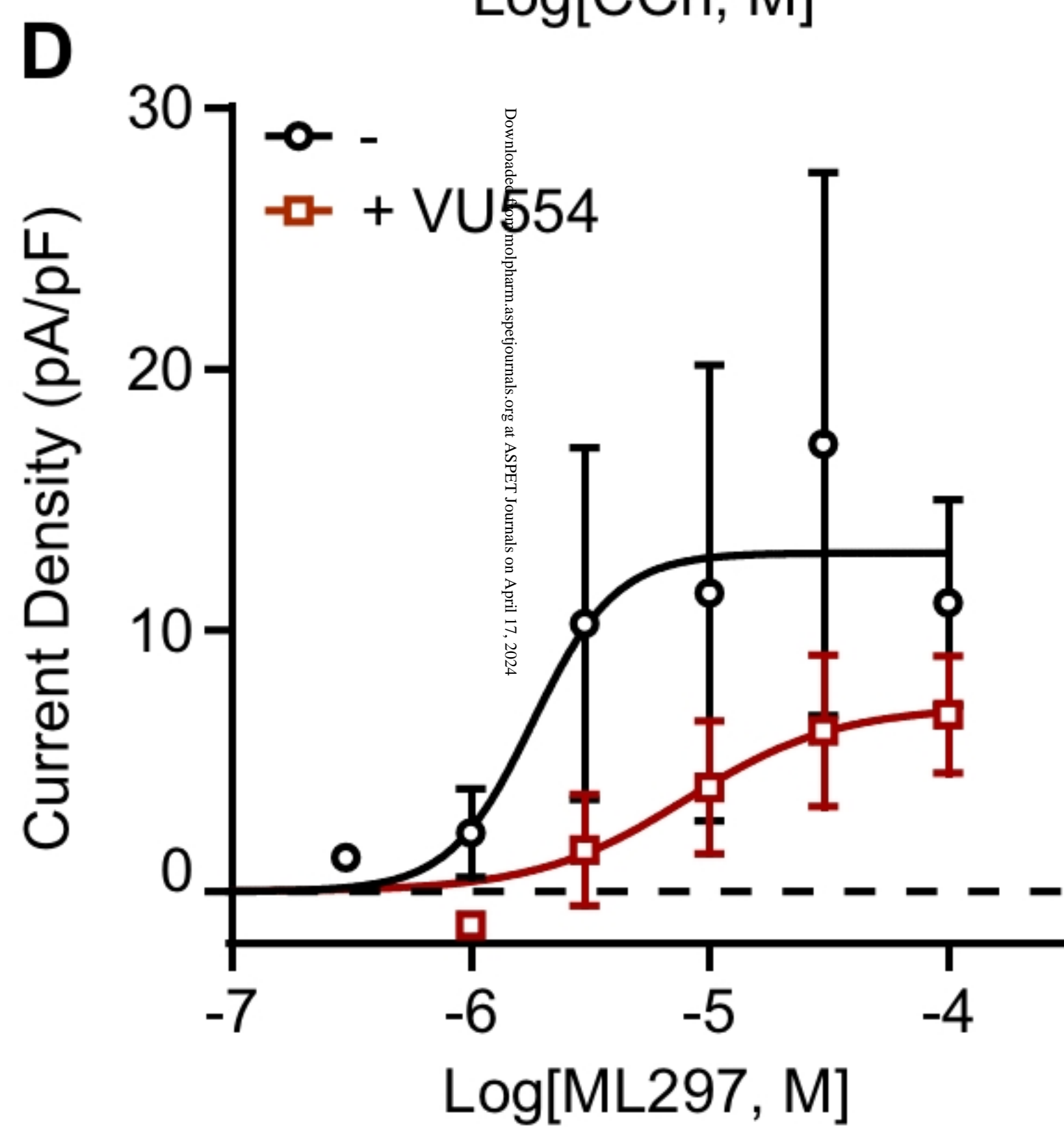
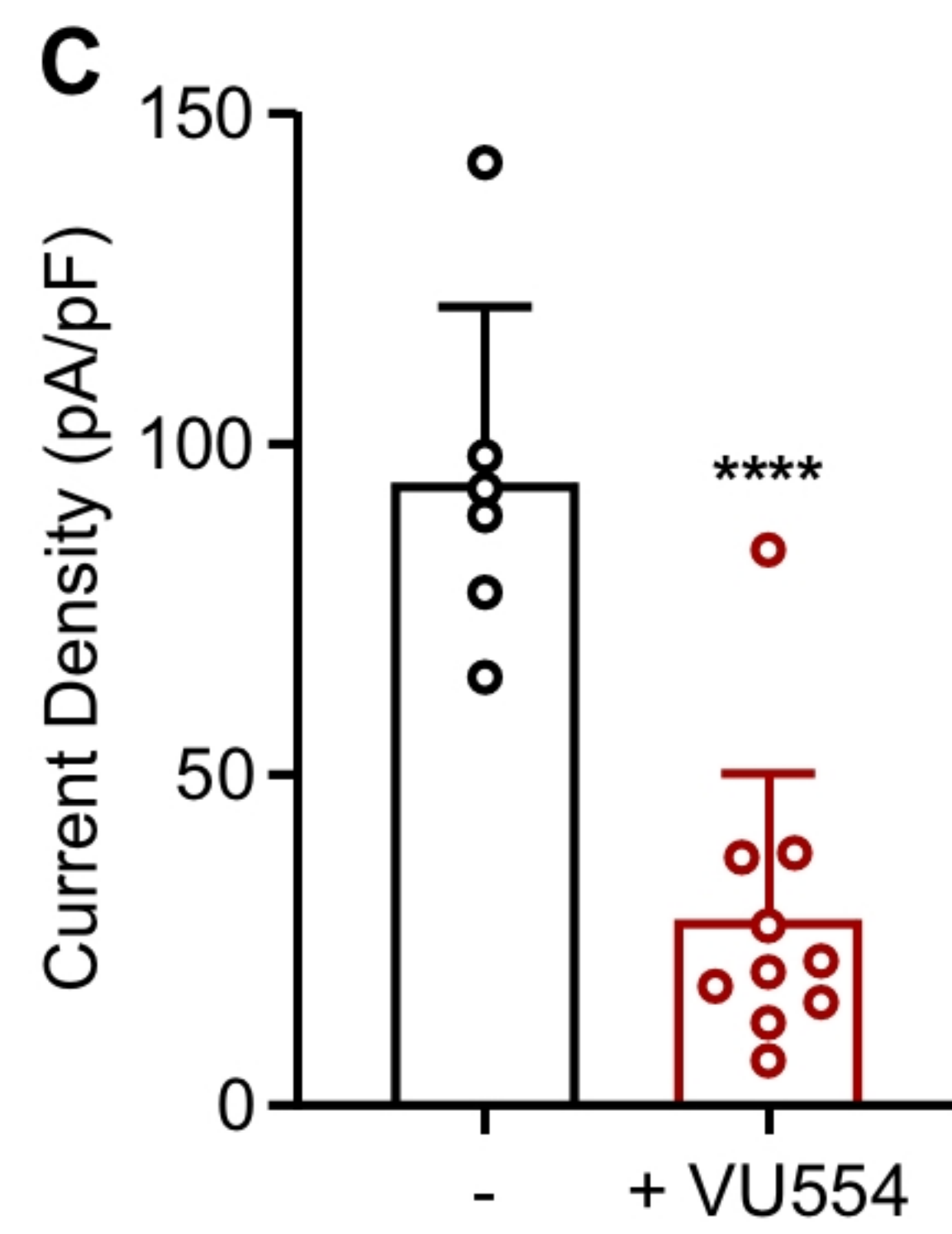
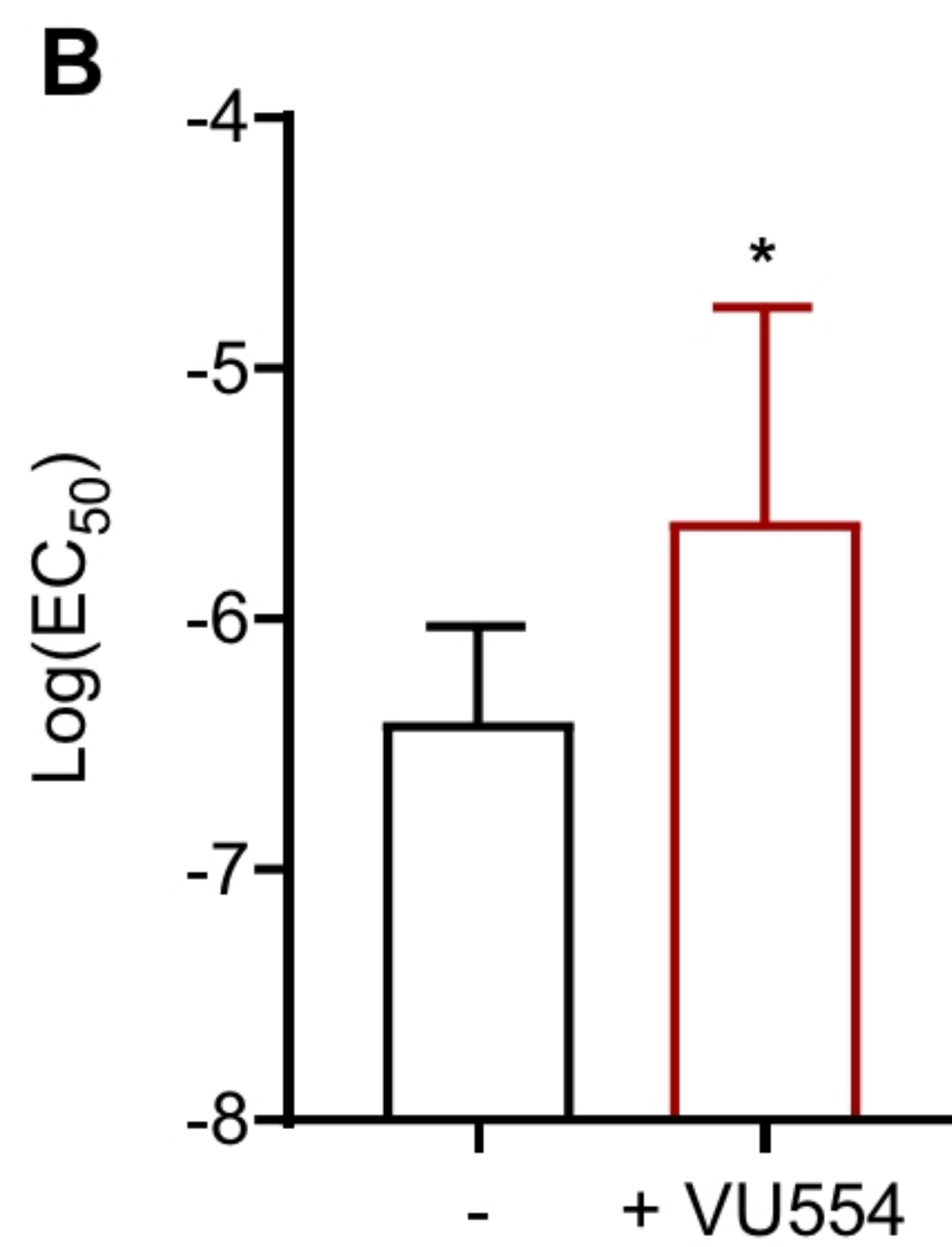
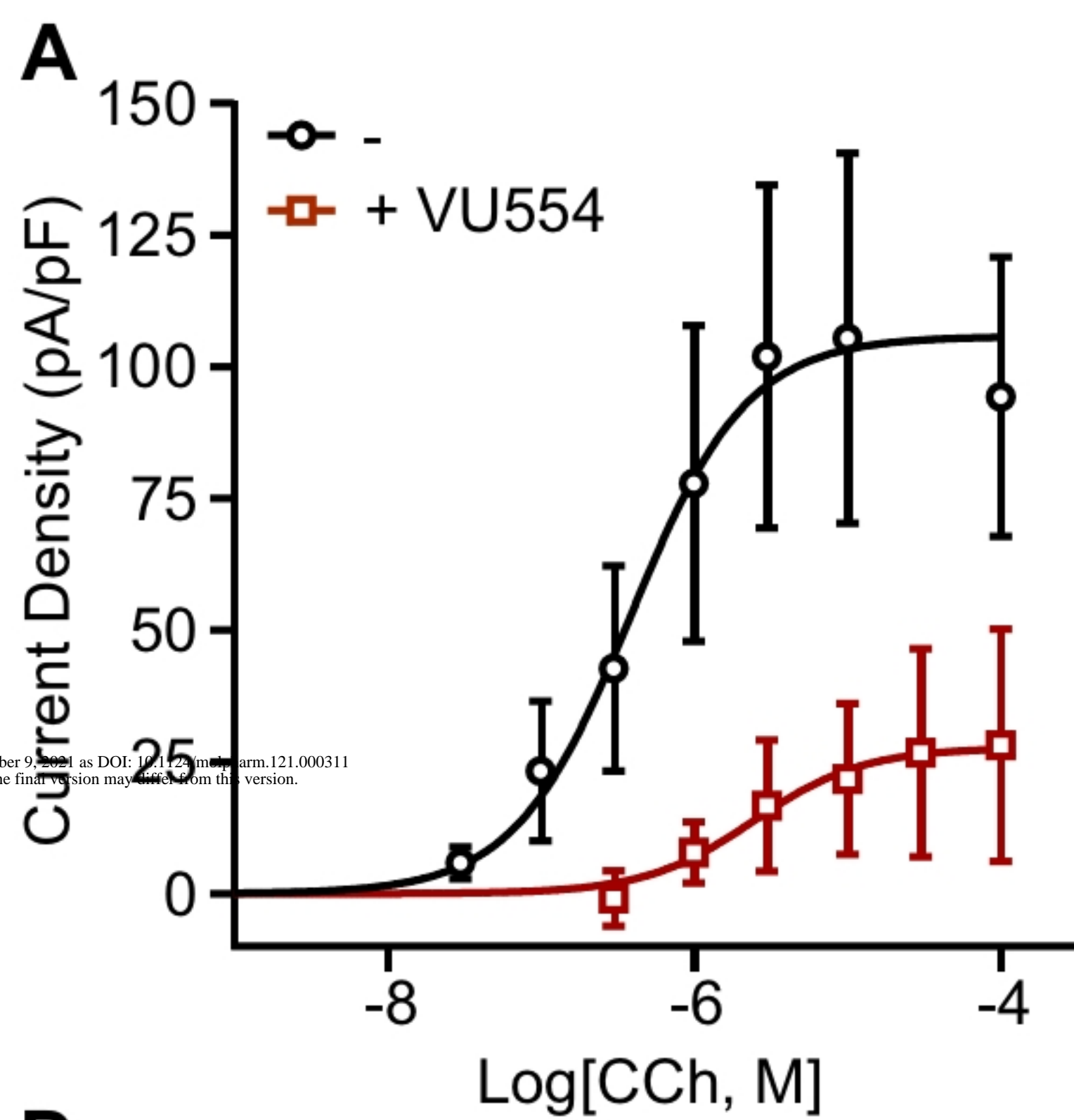




# FIGURE 4

Molecular Pharmacology Fast Forward. Published on September 9, 2021 as DOI: 10.1124/molpharm.121.000311  
This article has not been copyedited and formatted. The final version may differ from this version.

